

# Thermodynamically consistent nonlinear viscoplastic formulation with well-conditioned recovery of the inviscid solution: Theory and implicit integration algorithm with exact solution for the linear case

K. Nguyen<sup>a</sup>, Víctor J. Amores<sup>a</sup>, Francisco J. Montáns<sup>a</sup>

<sup>a</sup>*Escuela Técnica Superior de Ingeniería Aeronáutica y del Espacio, Universidad Politécnica de Madrid, Pza. Cardenal Cisneros, 28040, Madrid*

---

## Abstract

In this work, a consistent viscoplasticity formulation is derived from thermodynamical principles and employing the concept of continuum elastic corrector rate. The proposed model is developed based on the principle of maximum viscoplastic dissipation for determining the flow direction. The model uses both the equivalent viscoplastic strain and its rate as state variables. Power balance and energy balance give, respectively, separate evolution equations for the equivalent viscoplastic strain rate and the viscoplastic strain, the former written in terms of inviscid rates. Several key points distinguish our formulation from other proposals. First, the viscoplastic strain rate (instead of a yield function) consistently distinguishes conservative from dissipative behaviours during reverse loading; and the discrete implicit integration algorithm is an immediate implementation of the continuum theory based on the mentioned principles. Second, the inviscid solution is recovered in a well-conditioned manner by simply setting the viscosity to zero. Indeed, inviscid plasticity, viscoelasticity and viscoplasticity are particular cases of our formulation and integration algorithm, and are recovered just by setting the corresponding parameters to zero (viscosity or yield stress). Third, the linear viscoplasticity solution is obtained in an exact manner for proportional loading cases, independently of the time step employed. Four, general nonlinear models (Perzyna, Norton, etc) may be immediately incorporated as particular cases both in the theory and the computational implementation.

**Keywords:** Viscoplasticity, plasticity, viscoelasticity, consistency viscoplastic model, Perzyna model, Duvaut-Lions model.

---

## 1. Introduction

The elastoplastic behavior of materials have a time-dependent component, meaning that the speed at which plastic dissipation takes place affects the observed behavior. This time-dependent effect is usually modelled through a viscoplastic constitutive relation. In many

---

*Email addresses:* [khanhnguyen.gia@upm.es](mailto:khanhnguyen.gia@upm.es) (K. Nguyen), [victorjesus.amores@upm.es](mailto:victorjesus.amores@upm.es) (Víctor J. Amores), [fco.montans@upm.es](mailto:fco.montans@upm.es) (Francisco J. Montáns )

cases, when the rate of loading is very small and the time-dependent effect can be neglected, the rate-independent elastoplasticity models can provide a good approximation to the experimental results [1, 2]. However, in the cases when such conditions are not met, the rate-dependency is important, and must be taken into account in the constitutive model to obtain accurate predictions. In a general purpose model, the importance of such effects cannot be determined apriori, so a smooth transition in the simulations from rate-independent to rate-dependent plasticity is desired. Viscoplasticity is the common type of model incorporating strain-rate dependent plastic flow. Furthermore, it is desirable to also incorporate viscoelasticity in the same framework.

Many constitutive viscoplastic models have been presented, including their dedicated computational treatments. In general, the viscoplasticity models can be classified into two families. One is the so-called *overstress* models; the other family comprises the so-called *consistency* models. The first family is based on the ideas proposed by Perzyna [3], in which the current stress state can be outside the yield surface and the yield function may be greater than zero (hence, the *overstress* name). In these cases, the Kuhn-Tucker conditions typical of plasticity are not applicable. The rate of an equivalent (visco-)plastic strain  $\dot{\gamma}$  is obtained from a direct evolution equation in terms of the overstress and the viscosity  $\eta$ ; this rate is incrementally integrated to obtain the equivalent (visco-)plastic strain  $\gamma$ . The Perzyna model [3] and the Duvaut-Lions model [4], among others, are the most popular formulations in this first family. Both models are not only widely used in small strain problems [5, 6, 7, 8, 9, 10, 11, 12, 13], but have also been extended to finite strain problems [14, 15, 16, 17] and are common also in crystal plasticity, often tailored and referred to as power-laws [18, 19]. Nonetheless, despite the improvements and advances in their computational treatments [5, 6, 7, 8, 9, 10, 11, 13], both models still present limitations. The major drawback of the Perzyna model is that this model has an ill-conditioned inviscid limit [20] and because of its inherent structure, it may not naturally converge to the inviscid solution when the viscosity tends to zero for non-smooth multi-surface viscoplasticity [8, 21], a key aspect in crystal plasticity. The Duvaut-Lions model has the advantage compared with the Perzyna model in that it can be combined with a non-smooth yield surface, and the formulation naturally incorporates the inviscid limit as part of the solution. In this model, the trial and the inviscid solutions are computed first and then the viscous solution is determined as a relaxation of the trial state to the inviscid solution, a relaxation which depends on the characteristic (relaxation) time. However, the advantage is sometimes seen as a handicap respect to Perzyna's model, because it must be used in conjunction with a separate integration algorithm for the inviscid elastoplastic rate equations, where the evolution rule is needed for the yield surface, in case of hardening or softening plasticity [8]. But more importantly, in principle the Duvaut-Lions model does not incorporate general relations of the Perzyna type, being restricted to linear viscoplasticity, so it is seldom used when the rate-independent solution is not important and the viscous contribution is expected to be relevant.

The second family of viscoplasticity models has been introduced by Wang et al. [22] and then further explored by many authors [23, 24, 25, 26]. This approach includes the viscoplastic behaviour by incorporating the time-dependency in a so-called *rate-dependent yield surface*; the purpose being that the Kuhn-Tucker conditions, typical of rate independent plasticity, remain valid. The viscoplastic multiplier is determined from a non-homogeneous differential

equation derived from the consistency condition at the rate-dependent yield surface, so these models are referred to as the “consistency models”. The elastic domain in the stress  $\boldsymbol{\sigma}$ -space is defined as  $\mathbb{E}_{\boldsymbol{\sigma}} = \{\boldsymbol{\sigma} \in \mathbb{S} \mid f(\boldsymbol{\sigma}, \gamma, \dot{\gamma}) \leq 0\}$ , meaning that in the unloading case, the consistency model always unloads elastically [25] and  $f(\boldsymbol{\sigma}, \gamma, \dot{\gamma}) = 0$  is the viscoplastic yield function. This implies that the rate-dependent yield surface remains fixed during the unloading phase; in other words, the viscoplastic multiplier ( $\dot{\gamma}$ ) is not changed during unloading and is greater than zero (see e.g. Secs. 2.2 and 3.2 of [25]). In essence, this type of models presents the contradiction that at unloading detected by  $f(\boldsymbol{\sigma}, \gamma, \dot{\gamma}) \leq 0$ , plastic flow stops suddenly producing conservative behaviour with frozen  $\dot{\gamma} > 0$ , values which are inherent to a dissipative process. Hence, these formulations seem just motivated by numerical difficulties, but result in contradictory physical conditions.

In this paper, we introduce a novel thermodynamically motivated consistent viscoplastic formulation which naturally includes a well-conditioned recovery of the inviscid solution by simply setting the viscosity  $\eta = 0$ . The model avoids the limitations of the previous models, but incorporates their advantageous features, including general nonlinear viscosities and hardening. Furthermore, our proposal is not just a numerical convenience, but it is motivated in a proper implementation of physical principles. Indeed, our proposal is postulated from the principle of maximum dissipation in a straightforward manner, from which a function  $f(\boldsymbol{\sigma}, \gamma, \dot{\gamma})$  is obtained as a consequence of power conservation (not from a postulate) to include the rate dependence. Power balance and energy balance give, respectively, separate evolution equations for the viscoplastic strain rate and for the viscoplastic strain. This separation allows for the integration of plasticity, viscoplasticity, and viscoelasticity in a single computational setting, because plastic strain evolution and its rate are different variables with their own evolution equations, each one dominating the particular cases of inviscid plasticity or viscoelasticity. Unlike the consistency model proposed by Wang et al. [22], in our model the trial viscoplastic multiplier  $\dot{\gamma}$  is used consistently to check whether either dissipation or conservative behavior occurs. As a result, dissipation can still be generated during the “unloading” phase ( $f(\boldsymbol{\sigma}, \gamma, \dot{\gamma}) < 0$ ), until  $\dot{\gamma}$  vanishes, even when the trial state lies inside the inviscid yield function. This viscoplastic rate is obtained from an evolution equation in rate form in terms of inviscid rates. Whereas in the continuum theory we show that power balance results in energy balance by integration, in the discrete general theory, both principles facilitate different equations to compute  $\Delta\dot{\gamma}$  and  $\Delta\gamma$ . The formulation may accommodate most of the nonlinear uniaxial viscoplastic models such as Perzyna, Duvaut-Lions and Norton-type power laws, etc.

An implicit integration algorithm derived immediately from the continuum theory, based on the novel framework employing continuum elastic rate correctors, is also proposed including general nonlinear viscoplasticity [27]. The exact solution, independent of the time increment employed, is recovered for linear small strain  $J_2$ -viscoplasticity under proportional loading (as for the case of linear elastoplasticity). We compare results with some of the well-known viscoplastic models such as the Perzyna, the Duvaut-Lions and the consistency models. We focus on the ideas behind the proposal, so we employ in the presentation infinitesimal strains. A large strains implementation using a framework with logarithmic strains, a multiplicative decomposition of the deformation gradient and the continuum elastic corrector rates framework is simple, being the algorithmic difficulty just related to the kinematic mappings,

see e.g. [28, 29, 30] for this type of formulations, and [31] for a simple large-strain plane-stress implementation of this type of approach. Finally, finite element non-homogeneous numerical examples are presented using our model to demonstrate its numerical implementation and the computational efficiency of our proposal.

## 2. Derivation of the model from thermodynamic principles

### 2.1. Dissipation inequality

In this section we establish the basic equations of the consistency viscoplastic model based on the rheological model shown in Figure 1. This rheological model is well-known as the Bingham model, which motivates many viscoplastic formulations. Noteworthy, the Bingham model recovers the Maxwell viscoelasticity rheological model if the yield stress vanishes, and it recovers the Prandtl plasticity rheological model if the viscosity vanishes. Then, such cases should be naturally recovered both by the continuum theory and by the integration algorithm simply setting the respective constants to zero. Unfortunately, this is not the usual case in the literature.

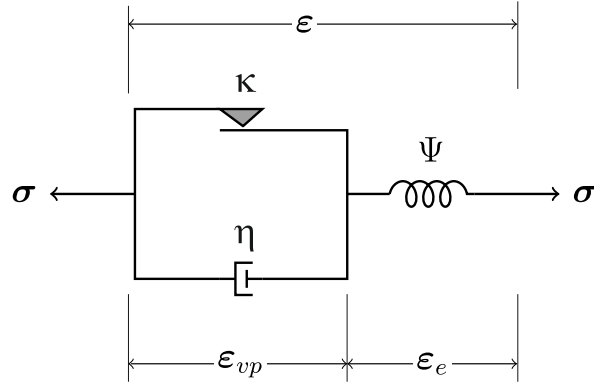


Figure 1: Rheological model for viscoplasticity.

The rheological model element considers two strain-like internal variables,  $\epsilon_e$  as the elastic strain governing the conservative behaviour through  $\Psi_{int}(\epsilon_e) \equiv \Psi(\epsilon_e)$  and  $\epsilon_{vp}$ , as a viscoplastic strain common to both the friction and the damper element and, hence, governing the dissipative behaviour. It also considers an external strain variable  $\epsilon$ , a result of the external work. We focus on conservation principles, so we consider the explicit dependencies given by  $\epsilon_e(\epsilon, \epsilon_{vp})$ , which results, by straightforward use of the chain rule, in

$$\dot{\epsilon}_e = \frac{\partial \epsilon_e}{\partial \epsilon} : \dot{\epsilon} + \frac{\partial \epsilon_e}{\partial \epsilon_{vp}} : \dot{\epsilon}_{vp} =: {}^{tr}\dot{\epsilon}_e + {}^{ct}\dot{\epsilon}_e \quad (1)$$

where, note,  ${}^{tr}\dot{\epsilon}_e$  and  ${}^{ct}\dot{\epsilon}_e$  refer, respectively, to trial and corrector *continuum rates* of the elastic strain, not to algorithmic ones. The infinitesimal strains in this presentation, based on elastic corrector rates, facilitate an immediate extension to finite strains based on the multiplicative decomposition preserving the additive structure; see [27, 28, 29]. If

$\mathcal{P} = \boldsymbol{\sigma} : \dot{\boldsymbol{\varepsilon}}$  is the external power and  $\dot{\Psi}$  is the change rate of the stored energy, by definition, the dissipation power is

$$\mathcal{D}^p \equiv \mathcal{P} - \dot{\Psi} = \boldsymbol{\sigma} : \dot{\boldsymbol{\varepsilon}} - \frac{d\Psi(\boldsymbol{\varepsilon}_e)}{d\boldsymbol{\varepsilon}_e} : \dot{\boldsymbol{\varepsilon}}_e \quad (2)$$

$$= \boldsymbol{\sigma} : \dot{\boldsymbol{\varepsilon}} - \frac{d\Psi(\boldsymbol{\varepsilon}_e)}{d\boldsymbol{\varepsilon}_e} : (\text{tr} \dot{\boldsymbol{\varepsilon}}_e + {}^{ct}\dot{\boldsymbol{\varepsilon}}_e) \geq 0 \quad (3)$$

where in Eq. (3) we used Eq. (1). Now, following the typical Coleman arguments [32], we analyse the two different cases (namely, the conservative and dissipative components of the power  $\mathcal{P} = \dot{\Psi} + \mathcal{D}^p$ ):

- *Conservative case:* In the case of absence of dissipation,  $\dot{\boldsymbol{\varepsilon}}_{vp} = \mathbf{0} = - {}^{ct}\dot{\boldsymbol{\varepsilon}}_e$ , and

$$\mathcal{D}^p = \boldsymbol{\sigma} : \dot{\boldsymbol{\varepsilon}} - \frac{d\Psi(\boldsymbol{\varepsilon}_e)}{d\boldsymbol{\varepsilon}_e} : \frac{\partial \boldsymbol{\varepsilon}_e}{\partial \boldsymbol{\varepsilon}} : \dot{\boldsymbol{\varepsilon}} \equiv 0 \quad (4)$$

which must hold for any arbitrary  $\dot{\boldsymbol{\varepsilon}}$ , so necessarily—note the abuse of notation in keeping the same symbol for the functions regardless of their arguments

$$\boldsymbol{\sigma} = \frac{\partial \Psi(\boldsymbol{\varepsilon}, \boldsymbol{\varepsilon}_{vp})}{\partial \boldsymbol{\varepsilon}} \equiv \frac{d\Psi(\boldsymbol{\varepsilon}_e)}{d\boldsymbol{\varepsilon}_e} : \frac{\partial \boldsymbol{\varepsilon}_e(\boldsymbol{\varepsilon}, \boldsymbol{\varepsilon}_{vp})}{\partial \boldsymbol{\varepsilon}} = \frac{d\Psi(\boldsymbol{\varepsilon}_e)}{d\boldsymbol{\varepsilon}_e} =: \boldsymbol{\sigma}^{|e} \quad (5)$$

where  $\partial \boldsymbol{\varepsilon}_e(\boldsymbol{\varepsilon}, \boldsymbol{\varepsilon}_{vp})/\partial \boldsymbol{\varepsilon} = \mathbb{I}^s$ , the fourth order fully symmetric identity tensor, is due to the additive setting that governs infinitesimal strains. At large strains this identification does not necessarily holds, but the concept of elastic corrector rate and its additive structure using logarithmic strains do, maintaining unaltered the additive structure of the infinitesimal theory and related algorithm at large strains [33, 34, 27]. Note also that in this infinitesimal case,  $\boldsymbol{\sigma}^{|e} := d\Psi/d\boldsymbol{\varepsilon}_e$  equals the stress tensor  $\boldsymbol{\sigma}$  obtained from external power balance in  $\boldsymbol{\sigma} : \dot{\boldsymbol{\varepsilon}}$ .

- *Purely dissipative case:* Using Eq. (5), the external power is frozen, i.e.  $\dot{\boldsymbol{\varepsilon}} = \mathbf{0}$ , so we have

$$\mathcal{D}^p = -\boldsymbol{\sigma} : {}^{ct}\dot{\boldsymbol{\varepsilon}}_e \quad (6)$$

Using the constraint of isochoric flow, the principle of maximum dissipation implies that [30]

$${}^{ct}\dot{\boldsymbol{\varepsilon}}_e = -c\dot{\gamma}\hat{\boldsymbol{n}} \quad (7)$$

where  $\hat{\boldsymbol{n}} = \boldsymbol{\sigma}^d / \|\boldsymbol{\sigma}^d\|$  is the associated constrained flow direction,  $\boldsymbol{\sigma}^d$  is the deviatoric stress and  $\|\boldsymbol{\sigma}^d\|$  is its norm, and  $c\dot{\gamma}$  is a multiplier. The constant  $c = \sqrt{3/2}$  is the scalar to account for uniaxial comparison so  $\dot{\gamma}$  takes the convenient uniaxial equivalence meaning; i.e. during a uniaxial test in the  $x$ -direction

$$({}^{ct}\dot{\boldsymbol{\varepsilon}}_e)_x = -\sqrt{\frac{2}{3}}c\dot{\gamma} \text{ so we take } c = \sqrt{\frac{3}{2}} \text{ to get } ({}^{ct}\dot{\boldsymbol{\varepsilon}}_e)_x = -\dot{\gamma} \quad (8)$$

For the classical infinitesimal case with isochoric flow, denoting the volumetric strain by  $\varepsilon_v = \text{tr}(\boldsymbol{\varepsilon}) = \text{tr}(\boldsymbol{\varepsilon}_e)$  and the deviatoric elastic one by  $\boldsymbol{\varepsilon}_e^d = \boldsymbol{\varepsilon}_e - \frac{1}{3}\varepsilon_v \mathbf{I}$ , we consider the stored energy function

$$\Psi(\boldsymbol{\varepsilon}_e) = \frac{1}{2}2\mu\boldsymbol{\varepsilon}_e^d : \boldsymbol{\varepsilon}_e^d + \frac{1}{2}K\varepsilon_v^2 \quad (9)$$

where  $\mu$  is the shear modulus and  $K$  is the bulk modulus. Using  $d\boldsymbol{\varepsilon}_e^d/d\boldsymbol{\varepsilon}_e = \mathbb{P}^d$ , the deviatoric projector, and  $d\boldsymbol{\varepsilon}_e^v/d\boldsymbol{\varepsilon}_e = \mathbf{I}$ , the identity tensor, the resulting trial stress rate is

$${}^{tr}\dot{\boldsymbol{\sigma}} \equiv {}^{tr}\dot{\boldsymbol{\sigma}}|^e := \frac{d\boldsymbol{\sigma}^{|e}}{d\boldsymbol{\varepsilon}_e} : {}^{tr}\dot{\boldsymbol{\varepsilon}}_e = \frac{d^2\Psi(\boldsymbol{\varepsilon}_e)}{d\boldsymbol{\varepsilon}_e \otimes d\boldsymbol{\varepsilon}_e} : {}^{tr}\dot{\boldsymbol{\varepsilon}}_e = \underbrace{2\mu}^{{}^{tr}\dot{\boldsymbol{\sigma}}^d} {}^{tr}\dot{\boldsymbol{\varepsilon}}_e^d + K\dot{\varepsilon}_v \mathbf{I} \quad (10)$$

and by Eq. (7), the corrector stress rate is

$${}^{ct}\dot{\boldsymbol{\sigma}} \equiv {}^{ct}\dot{\boldsymbol{\sigma}}|^e := \mathbb{C}_e : {}^{ct}\dot{\boldsymbol{\varepsilon}}_e = 2\mu {}^{ct}\dot{\boldsymbol{\varepsilon}}_e = -2\mu c\dot{\gamma}\hat{\mathbf{n}} \quad (11)$$

where  $\mathbb{C}_e := d^2\Psi(\boldsymbol{\varepsilon}_e)/d\boldsymbol{\varepsilon}_e \otimes d\boldsymbol{\varepsilon}_e$  is the elastic tangent. Because of the deviatoric nature of  $\hat{\mathbf{n}}$  we have  $\boldsymbol{\sigma} : \hat{\mathbf{n}} = \boldsymbol{\sigma}^d : \hat{\mathbf{n}}$ . Note that despite that we include herein the familiar rate forms for the infinitesimal case, the stresses are hyperelastic, i.e.

$$\boldsymbol{\sigma} \equiv \boldsymbol{\sigma}^{|e}(\boldsymbol{\varepsilon}_e) := \frac{d\Psi(\boldsymbol{\varepsilon}_e)}{d\boldsymbol{\varepsilon}_e} \quad (12)$$

so stress rate forms bellow are included just to facilitate the reader comparisons with other infinitesimal formulations. For the finite case, or for infinitesimal bi-modulus materials [35], direct hyperelastic relations are more convenient.

## 2.2. Thermodynamic consistency

Let us consider the aforementioned Bingham-Maxwell-Prandtl model, where a spring element, representing a stored energy, is in series with two dissipative elements in parallel (one friction and one damper). In the absence of external power (which requires  $\dot{\boldsymbol{\varepsilon}} = \mathbf{0}$ ), we must have the following relation from thermodynamic consistency (i.e. equivalence of the dissipation, or that the dissipated power equals the decrease rate of the stored energy for the case of frozen external power)

$$\mathcal{D}^p \equiv -\boldsymbol{\sigma} : {}^{ct}\dot{\boldsymbol{\varepsilon}}_e = \kappa(\gamma_p)\dot{\gamma}_p + g(\dot{\gamma}_v)\dot{\gamma}_v \geq 0 \quad (13)$$

where  $\gamma_p$  is the uniaxial-equivalent plastic strain (the cumulative sliding in the friction element) and  $\dot{\gamma}_v$  is the velocity of displacement in the damper. The functions  $\kappa(\gamma_p)$  and  $g(\dot{\gamma}_v)$  are the, possibly nonlinear, scalar uniaxial-equivalent functions representing the energy-conjugate stress-like internal variables in the friction and the damper elements, respectively. Furthermore, if both elements are in parallel, it is obvious that the kinematics imply that

$$\dot{\gamma}_p = \dot{\gamma}_v \equiv \dot{\gamma} = \frac{d\gamma}{dt} \quad (14)$$

Note that another implication of the description given by the rheological model is that the dissipation can be decoupled in an additive manner as described in the previous equations, separating the dependence on  $\gamma$  from that on  $\dot{\gamma}$ . With the above definitions and assumptions motivated from the rheological model, the equal sign identifying both versions of the dissipation in Eq. (13), states that

$$-\boldsymbol{\sigma} : {}^{ct}\dot{\boldsymbol{\varepsilon}}_e - \kappa(\gamma)\dot{\gamma} - g(\dot{\gamma})\dot{\gamma} = 0 \quad (15)$$

Then, using Eq. (7), the following two conditions must hold, the first one implying the first principle of thermodynamics (conservation of power by the identity in Eq. (13)) and the second one implying the non-negativity of dissipation from the second principle (the “ $\geq$ ” sign in Eq. (13))

$$\begin{cases} f\dot{\gamma} := [f_p(\boldsymbol{\varepsilon}_e, \gamma) - g(\dot{\gamma})]\dot{\gamma} := [c \boldsymbol{\sigma} : \hat{\mathbf{n}} - \kappa(\gamma) - g(\dot{\gamma})]\dot{\gamma} = 0 & \text{(first principle)} \\ \mathcal{D}^p := [\kappa(\gamma) + g(\dot{\gamma})]\dot{\gamma} \geq 0 & \text{(second principle)} \end{cases} \quad (16)$$

Note that from Eq. (12) we can write the dependencies either using the elastic strains as in  $f_p(\boldsymbol{\varepsilon}_e, \gamma)$  or using the stress as in  $f_p(\boldsymbol{\sigma}, \gamma)$ ; recall that to avoid proliferation of symbols, we use the same symbols for functions with a same physical meaning, regardless of the arguments (if convenient, we will write the relevant ones in the discussion, explicitly).

We usually require that the dissipation in both dissipative elements must be positive by themselves, i.e.  $\kappa(\gamma)\dot{\gamma} \geq 0$  and  $g(\dot{\gamma})\dot{\gamma} \geq 0$ , which is guaranteed if  $\kappa(\gamma) \geq 0$  and  $g(\dot{\gamma}) \geq 0$  and  $\dot{\gamma} \geq 0$ . In fact,  $\dot{\gamma} \geq 0$  is usually considered a requirement by definition (i.e.  $\gamma$  is a monotonically increasing variable). Then, from the first condition in Eq. (16), we have

- if  $\dot{\gamma} > 0$ , which corresponds to a dissipative case, the first principle implies

$$f(\boldsymbol{\varepsilon}_e, \gamma, \dot{\gamma}) \equiv f_p(\boldsymbol{\varepsilon}_e, \gamma) - g(\dot{\gamma}) \equiv c \boldsymbol{\sigma}(\boldsymbol{\varepsilon}_e) : \hat{\mathbf{n}}(\boldsymbol{\varepsilon}_e) - \kappa(\gamma) - g(\dot{\gamma}) = 0. \quad (17)$$

- if  $\dot{\gamma} = 0$ , which corresponds to a conservative case, we may have  $f = 0$ ,  $f > 0$  or  $f < 0$ . Now, we analyze the case that  $f > 0$ , from the fact that no dissipation is taken place and the viscoplastic strain is frozen ( $\dot{\gamma}_p = \dot{\gamma}_v = 0$ ). We assume that  $g(0) = 0$ ; no stress in the dashpot for  $\dot{\gamma}_v = 0$ . Then, the case  $f > 0$  requires

$$f(\boldsymbol{\varepsilon}_e, \gamma, \dot{\gamma}) \equiv f_p(\boldsymbol{\varepsilon}_e, \gamma) := c \boldsymbol{\sigma}(\boldsymbol{\varepsilon}_e) : \hat{\mathbf{n}}(\boldsymbol{\varepsilon}_e) - \kappa(\gamma) > 0 \quad (18)$$

However, by the definition in the rheological model,  $\kappa(\gamma)$  is the yield stress and by definition of the  $\hat{\mathbf{n}}$  symbol  $\boldsymbol{\sigma} : \hat{\mathbf{n}} > 0$ , so  $f_p > 0$  implies  $c \|\boldsymbol{\sigma}^d\| > \kappa(\gamma)$ . In turn this implies by equilibrium in the friction element an increment in the plastic strain,  $\dot{\gamma}_p > 0$ , which would be in contradiction with our original assumption for this case. Consequently by the definition of  $\kappa(\gamma)$ , the condition  $\dot{\gamma} = 0$  requires  $f = f_p \leq 0$  and the condition  $f > 0$  is not possible. Note that this condition is coincident with that of the inviscid (purely plastic) case.

$f_p(\boldsymbol{\varepsilon}_e, \gamma)$  in Eq. (18) is the classical plasticity (inviscid) criterion and  $f(\boldsymbol{\varepsilon}_e, \gamma, \dot{\gamma}) = 0$  can be interpreted as a “dynamic loading surface”, which changes during the deformation process by work-hardening effects and by the influence of the strain-rate effect, as shown in Figure 2.

### 2.3. Continuum theory

The previous equation implies that during the continuum flow with  $\dot{\gamma} > 0$  we must also have  $\dot{f} = 0$  regardless of the value of the other variables, so the requirement  $f = 0$  is





the previous Eq. (21) can be re-written as

$$\ddot{\gamma} + \frac{\dot{\gamma}}{\hat{\tau}} = \frac{\dot{\gamma}_\infty}{\hat{\tau}} \quad (24)$$

and taking  $\Gamma := \dot{\gamma}$  for now for notational convenience, the previous equation leads to a first-order *scalar* differential equation in  $\Gamma$ :

$$\dot{\Gamma} + \frac{\Gamma}{\hat{\tau}} = \frac{\dot{\gamma}_\infty}{\hat{\tau}} \quad (25)$$

Depending on the material parameters, the above equation could be a linear differential equation or a nonlinear differential equation. For developing the main ideas, we hereby particularize to the quite typical case in which  $\kappa' = H$  and  $g' = \eta$  are constant (e.g. a linear hardening and a constant viscosity  $\eta$ ). Then, the solution of Eq. (25) can be determined as follows, if we assume that also  $c\hat{\mathbf{n}} : \mathbb{C}_e : \dot{\boldsymbol{\varepsilon}}$  is constant (constant speed test, the case relevant for the incremental formulation below)

$$\begin{cases} \Gamma \equiv \dot{\gamma} = \dot{\gamma}_\infty = \frac{c\hat{\mathbf{n}} : \mathbb{C}_e : \dot{\boldsymbol{\varepsilon}}}{c^2\hat{\mathbf{n}} : \mathbb{C}_e : \hat{\mathbf{n}} + H} > 0 & \text{if } \eta = 0 \\ \Gamma \equiv \dot{\gamma} = \dot{\gamma}_\infty + \bar{C} \exp\left(-\frac{t}{\hat{\tau}}\right) > 0 & \text{if } \eta \neq 0 \end{cases} \quad (26)$$

where  $\bar{C}$  is a constant determined by  $\dot{\gamma}(t=t_0) =: \dot{\gamma}_0$  as  $\bar{C} = [\dot{\gamma}_0 - \dot{\gamma}_\infty] \exp(t_0/\hat{\tau})$ , so the second Equation (26) is

$$\dot{\gamma} = \underbrace{\dot{\gamma}_\infty}_{\substack{\text{“equilibrated”} \\ \text{(i.e. at } t \rightarrow \infty) \\ \text{or inviscid}}} + \underbrace{\overbrace{[\dot{\gamma}_0 - \dot{\gamma}_\infty]}^{\substack{\text{“non-equilibrium”} \\ \text{forcing rate}}} \exp\left(-\frac{t-t_0}{\hat{\tau}}\right)}_{\substack{\text{“non-equilibrium” rate} \\ \text{(viscous contribution)}}} \quad (27)$$

in which we can interpret that  $\dot{\gamma}_{neq} := \dot{\gamma}_0 - \dot{\gamma}_\infty$  is the non-equilibrated rate and  $\dot{\gamma}_\infty$  corresponds to the elastoplastic (inviscid) rate solution, i.e. the solution with  $\eta \rightarrow 0$  or at  $t \rightarrow \infty$ . Another physical interpretation typical of *viscoelasticity* is obtained rearranging terms

$$\dot{\gamma}(t) = \underbrace{\dot{\gamma}_0 \exp\left(-\frac{t-t_0}{\hat{\tau}}\right)}_{\text{I.C. vanishing term}} + \underbrace{\dot{\gamma}_\infty \left[1 - \exp\left(-\frac{t-t_0}{\hat{\tau}}\right)\right]}_{\text{Steady-state accommodating term}} \geq 0 \quad (28)$$

i.e. the first addend is the influence of the initial condition  $\dot{\gamma}_0$  vanishing in time, and the second term is the steady-state term  $\dot{\gamma}_\infty$  being enforced in time. Substitute Eq. (27) in Eq. (24) to get the speed at which this adaptation process takes place—namely the speed at which  $\dot{\gamma}_{neq}$  is cancelled-out

$$\ddot{\gamma}(t) = -\frac{\dot{\gamma}_{neq}}{\hat{\tau}} \exp\left(-\frac{t-t_0}{\hat{\tau}}\right) \quad (29)$$

Note that Eq. (29) is in essence similar to the Perzyna model but in second derivative and fully written in kinematic quantities, in rate form (consider that at  $t = t_0$  we have  $\ddot{\gamma} = -\dot{\gamma}_{neq}/\hat{\tau}$ ). Of course in the continuum theory, the incremental consistency parameter is obtained by integration of Eq. (27) from  $t = t_0$  to a time  $t$  as

$$\begin{aligned}\gamma &= \gamma_0 + \int_{t=t_0}^t \left[ \dot{\gamma}_\infty + \dot{\gamma}_{neq} \exp\left(-\frac{t-t_0}{\hat{\tau}}\right) \right] dt \\ &= \gamma_0 + \dot{\gamma}_\infty (t - t_0) + \hat{\tau} (\dot{\gamma}_0 - \dot{\gamma}_\infty) \left[ 1 - \exp\left(-\frac{t-t_0}{\hat{\tau}}\right) \right]\end{aligned}\quad (30)$$

where

$$\int_{t_0}^t \exp\left(-\frac{t-t_0}{\hat{\tau}}\right) dt = -\hat{\tau} \exp\left(-\frac{t-t_0}{\hat{\tau}}\right) \Big|_{t_0}^t = \hat{\tau} \left[ 1 - \exp\left(-\frac{t-t_0}{\hat{\tau}}\right) \right] =: \hat{\tau} \xi(t - t_0) \quad (31)$$

is a result that we will use repeatedly below with  $\xi(t - t_0)$  as compact notation. A relevant case is when a sudden relaxation takes place. In this case, taking  $t_0 = 0$ ,  $\gamma_0 \neq 0$ ,  $\dot{\gamma}_0 \neq 0$ ,  $\dot{\gamma}_\infty = 0$ ,  $t \rightarrow \infty$ , we get the value at equilibrium, namely  $\gamma = \gamma_0 + \hat{\tau} \dot{\gamma}_0 =: \gamma_\infty^r$ ; i.e. the equilibrium viscoplastic strain  $\gamma_\infty^r$  is  $\hat{\tau} \dot{\gamma}_0$  away from  $\gamma_0$ .

In the viscoplastic case, we do not use any unloading/reloading condition as in plasticity. However, there are two similar cases: conservative case and dissipative case. The condition for conservative case is simply physically determined by  $\dot{\gamma} = 0$ , in which case we may have  $f \neq 0$  and  $\dot{f} \neq 0$ , but also  $f = 0$ . The condition for dissipative case simply requires  $\dot{\gamma} > 0$ , which implies that  $f = \dot{f} = 0$  by the first principle. The case  $\dot{\gamma} < 0$  is not possible by definition (would entail a negative dissipation, violating the second law of thermodynamics). Both conservative and dissipative cases are distinguished by  $\dot{\gamma}$ , not by  $f$ ; i.e. it is  $\dot{\gamma}$ , computed from its own evolution Equation (27) the quantity to check, and its numerical integration must just guarantee that  $f \not\geq 0$ . However, the start of viscoplastic loading from elastic one is detected by  $f_p > 0$ .

In order to obtain the continuous viscoplastic tangent moduli tensor, we can use the constitutive equation in the rate form along Eq. (28)

$$\begin{aligned}\dot{\boldsymbol{\sigma}} &= \mathbb{C} : \dot{\boldsymbol{\varepsilon}} = \mathbb{C}_e : \dot{\boldsymbol{\varepsilon}}_e = \mathbb{C}_e : (\text{}^{tr}\dot{\boldsymbol{\varepsilon}}_e + \text{}^{ct}\dot{\boldsymbol{\varepsilon}}_e) = \mathbb{C}_e : (\dot{\boldsymbol{\varepsilon}} - c\dot{\gamma}\hat{\mathbf{n}}) \\ &= \left[ \mathbb{C}_e - \xi(t - t_0) \frac{(\mathbb{C}_e : \hat{\mathbf{n}}) \otimes (\mathbb{C}_e : \hat{\mathbf{n}})}{\hat{\mathbf{n}} : \mathbb{C}_e : \hat{\mathbf{n}} + \kappa'/c^2} \right] : \dot{\boldsymbol{\varepsilon}} - c\dot{\gamma}_0 \exp\left(-\frac{t-t_0}{\hat{\tau}}\right) \mathbb{C}_e : \hat{\mathbf{n}}\end{aligned}\quad (32)$$

If the initial condition is  $\dot{\gamma}_0 = 0$ , the last addend vanishes, so Eq. (32) is

$$\dot{\boldsymbol{\sigma}} = \underbrace{\left[ \mathbb{C}_e - \frac{\mathbb{C}_e : \hat{\mathbf{n}} \otimes \mathbb{C}_e : \hat{\mathbf{n}}}{\hat{\mathbf{n}} : \mathbb{C}_e : \hat{\mathbf{n}} + \kappa'/c^2} \xi(t - t_0) \right]}_{\mathbb{C}} : \dot{\boldsymbol{\varepsilon}} \quad (33)$$

where  $\mathbb{C}$  denotes the continuous viscoplastic tangent modulus tensor. Note that  $\mathbb{C}$  is bounded by the elastic tangent modulus tensor for the instantaneous response ( $t = t_0$  and  $\xi(t_0) = 0$ ),

and by the elastoplastic tangent modulus tensor for the long term response ( $t \rightarrow \infty$  and  $\xi(\infty) \rightarrow 1$ ), that is

$$\mathbb{C} = \begin{cases} \mathbb{C}_e & \text{for } t \rightarrow t_0 \text{ or } \eta \rightarrow \infty \\ \mathbb{C}_e - \frac{\mathbb{C}_e : \hat{\mathbf{n}} \otimes \mathbb{C}_e : \hat{\mathbf{n}}}{\hat{\mathbf{n}} : \mathbb{C}_e : \hat{\mathbf{n}} + \kappa'/c^2} \equiv \mathbb{C}_{ep} & \text{for } t \rightarrow \infty \text{ or } \eta \rightarrow 0 \end{cases} \quad (34)$$

Obviously, in the cases in which the coefficients of the differential equation are not constant, the solution depends on those functions, but the previous expressions may be considered as an approximation if that nonlinearity is weak or the computational steps, small. A general algorithmic solution, including nonlinear functions, is given below.

#### 2.4. Proportional loading cases

Several monotonic, uniaxial cases are of interest to understand the behaviour of the model, so they are briefly discussed here for the linear case.

##### 2.4.1. Constant rate loading case

The first case is when  $\dot{\epsilon}$  is a constant uniaxial loading (i.e. 1D). In this case, until  $f_p > 0$  at  $t > t_0$ , the stress rate is  $\dot{\sigma} = E\dot{\epsilon}$ , where  $E$  is the Young modulus and  $\dot{\sigma}$  is the uniaxial stress rate. Once  $f_p > 0$ , if there is no hardening ( $\kappa' = H = 0$ ), since  $\dot{\gamma}_0 = 0$  at  $t_0$  (onset of viscoplastic loading), the 1D version of Eq. (32) results in

$$\dot{\sigma} = E\dot{\epsilon} - E\dot{\epsilon} \left[ 1 - \exp \left( -\frac{t - t_0}{\hat{\tau}} \right) \right] \quad (35)$$

with  $\hat{\tau} = \eta/E$ . Note that for  $t = t_0$  we have the elastic  $\dot{\sigma} = E\dot{\epsilon}$  and for  $t \rightarrow \infty$  we have  $\dot{\sigma} = 0$ , which is the rate of the perfect plasticity solution. The integral from  $t = t_0$  to  $t$  is

$$\sigma - \kappa_0 = \int_{t_0}^t \dot{\sigma} dt = \hat{\tau} E \dot{\epsilon} \xi(t - t_0) = \eta \dot{\gamma}_\infty \xi(t - t_0) \quad (36)$$

giving the limits  $\sigma = \kappa_0$  for  $t = t_0$  and  $\sigma = \kappa_0 + \eta \dot{\gamma}_\infty$  for  $t \rightarrow \infty$ . This is shown in Fig. 3a. The effect in this figure of increasing  $\eta$  is the same as increasing the rate  $\dot{\epsilon} = \dot{\gamma}_\infty$ .

For the case of simple shear, the shear stress  $\sigma_s$  is computed in terms of the tensorial shear strain  $\epsilon_s$  (half the engineering one) from the 3D solution, Eq. (32), as

$$\sigma_s - \frac{1}{\sqrt{3}}\kappa_0 = \int_{t_0}^t \dot{\sigma}_s dt = \hat{\tau} 2\mu \dot{\epsilon}_s \xi(t - t_0) = \frac{\eta}{c^2} \dot{\epsilon}_s \xi(t - t_0) \quad (37)$$

where we used  $\dot{\epsilon} = \dot{\epsilon}_s \hat{\mathbf{n}}$  and  $\mathbb{C}_e : \hat{\mathbf{n}} = 2\mu \hat{\mathbf{n}}$  and  $\hat{\mathbf{n}} : \mathbb{C}_e : \hat{\mathbf{n}} = 2\mu$  and  $\dot{\gamma}_\infty = c 2\mu \dot{\epsilon}_s / (2\mu c^2) = \dot{\epsilon}_s / c$  and  $\hat{\tau} = \eta / (2\mu c^2)$ . Then  $\sigma_s = \kappa_0 / \sqrt{3} + (\eta / c^2) \dot{\epsilon}_s \xi(t - t_0)$ .

The case with linear hardening shown in Fig. 3b is similar. Recall the definition of the relaxed viscoplastic strain  $\gamma_\infty^r := \gamma + \hat{\tau} \dot{\gamma}$  where the first addend is the current viscoplastic strain and the second one is its potential increment if a sudden relaxation process takes place.

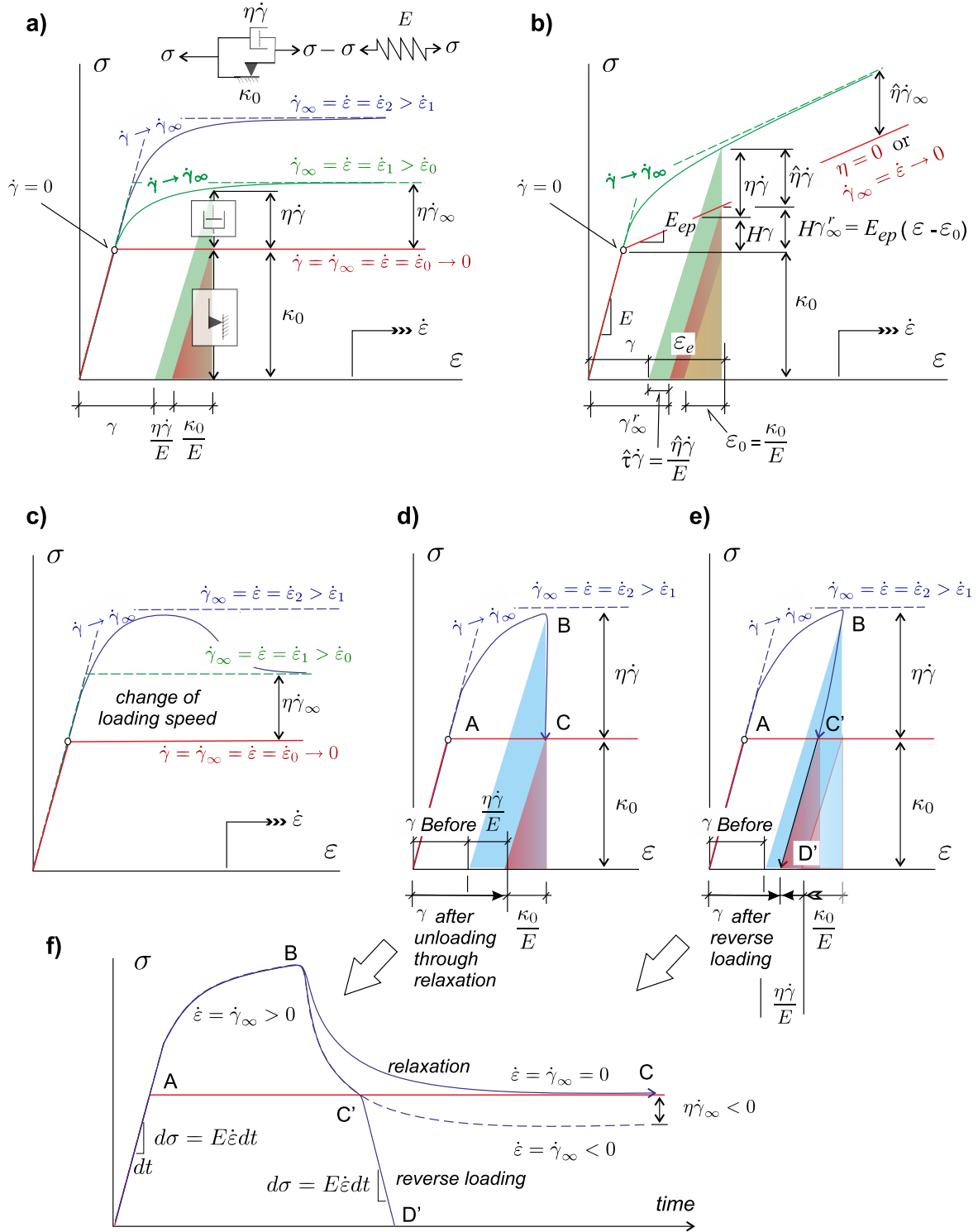


Figure 3: Uniaxial proportional loading. a) Monotonic loading at constant speed with no hardening. b) Monotonic loading at constant speed with hardening. c) Change of speed during monotonic loading. d) Viscous relaxation. e) Reverse loading/unloading. f) Stress versus time in relaxation and reverse-loading cases.

Define  $\hat{\eta} := \hat{\tau}E$ , so  $\hat{\eta} = [E/(E+H)]\eta$ , i.e.  $\eta = \hat{\eta}$  if no hardening is present. Recall that  $\dot{\gamma} = \dot{\gamma}_\infty \xi(t-t_0)$  with  $\dot{\gamma}_\infty = (E\dot{\varepsilon})/(E+H)$  for  $\dot{\gamma}_0 = 0$ . Then

$$\sigma - \kappa_0 = E_{ep} [\varepsilon(t) - \varepsilon_0] + \eta_{u-eq} \dot{\varepsilon} \xi(t-t_0) \quad (38)$$

$$\begin{aligned} &= E_{ep} [\varepsilon(t) - \varepsilon_0] + \hat{\eta} \dot{\gamma}_\infty \xi(t-t_0) \\ &= H\gamma_\infty^r + \hat{\eta} \dot{\gamma}(t) = H\gamma + \eta \dot{\gamma}(t) \end{aligned} \quad (39)$$

so  $\sigma = \kappa_0 + H\gamma_\infty^r + \hat{\eta} \dot{\gamma}(t) = \kappa_0 + H\gamma + \eta \dot{\gamma}(t)$ , and where we defined an equivalent uniaxial viscosity for the hardening case as  $\eta_{u-eq} = \eta E^2 / (E+H)^2 = \hat{\eta} E / (E+H)$  and  $E_{ep} = HE / (E+H)$ . In Eq. (39), the first identity is written in terms of yield stress at equilibrium ( $\kappa_0 + H\gamma_\infty^r$ ), see Fig. 2, whereas the second one is written in terms of the current one ( $\kappa_0 + H\gamma$ ). Note that

$$\frac{d\sigma}{d\varepsilon}(t \rightarrow \infty) = E_{ep} \quad (40)$$

as expected from Eq. (34). The sketch in Fig. 3b is better interpreted in terms of the quantities at equilibrium. Note that during relaxation with  $\dot{\varepsilon} = 0$  we have  $\gamma \rightarrow \gamma_\infty^r$ , and  $\varepsilon_e$  decreases by  $(\hat{\eta}/E) \dot{\gamma} = \hat{\tau} \dot{\gamma}$ . Here  $\hat{\eta}$  compensates for the hardening, because part of the stress in the dashpot  $\eta \dot{\gamma}$  will be absorbed by hardening. Then, the stress-strain curve is initially the same as the elastic one  $E$ , until  $\sigma = \kappa_0$ . Thereafter it will exponentially adapt to a line with slope  $E_{ep}$ , but shifted a constant  $\hat{\eta} \dot{\gamma}_\infty \equiv \eta_{u-eq} \dot{\varepsilon}$  from the elastoplastic one.

The case of simple shear may be obtained again directly from the 3D case taking  $\dot{\varepsilon} = \dot{\varepsilon}_s \hat{\mathbf{n}}$  and  $\mathbb{C}_e : \hat{\mathbf{n}} = 2\mu \hat{\mathbf{n}}$  and  $\hat{\mathbf{n}} : \mathbb{C}_e : \hat{\mathbf{n}} = 2\mu$  and  $\hat{\tau} = \eta / (2\mu c^2 + H)$ . In this case

$$\sigma_s - \frac{1}{\sqrt{3}} \kappa_0 = \int_{t_0}^t \dot{\sigma}_s dt = 2\mu_{ep} [\varepsilon_s(t) - \varepsilon_{0s}] + \frac{\eta_{s-eq}}{c^2} \dot{\varepsilon}_s \xi(t-t_0) \quad (41)$$

where we defined  $\eta_{s-eq} := \eta (2\mu)^2 / (2\mu + H/c^2)^2$  and  $2\mu_{ep} := 2\mu H / (2\mu c^2 + H)$ . Note that for  $H = 0$  we have  $\eta_{s-eq} = \eta$ , and that, also as expected from Eq. (34)

$$\frac{d\sigma}{d\varepsilon_s}(t \rightarrow \infty) = 2\mu_{ep} \quad (42)$$

Then, the shear stress versus shear strain (tensorial) has an initial (elastic) slope of  $2\mu$  until  $\sigma_s = \kappa_0/\sqrt{3}$  and a limiting slope of  $2\mu_{ep}$  for  $t \rightarrow \infty$ ; and an offset from the hardened elastoplastic line of  $\eta_{s-eq} \dot{\varepsilon}_s$  enforced progressively through the exponential-type function  $\xi(t-t_0)$ .

#### 2.4.2. Change of speed

If there is a change of speed, the stress path simply changes the horizontal asymptote, as shown in Fig. 3c, because  $\dot{\gamma}_\infty$  also does.

#### 2.4.3. Relaxation, unloading and reverse loading

In the case of sudden stop in strain loading, i.e.  $\dot{\varepsilon} = 0$ , a relaxation process occurs to the inviscid as shown in Fig. 3d and in Fig. 3f in time. The unloading curve in this latter case is

$$\sigma = \kappa_0 + \eta \dot{\gamma} = \kappa_0 + \eta \dot{\gamma}_0 \exp\left(-\frac{t-t_0}{\hat{\tau}}\right) \quad (43)$$

where  $\dot{\gamma}_0$  is the value at the beginning of the relaxation process and  $t_0$  is the instant at which relaxation begun. The tangent of the relaxation in time is

$$\frac{d\sigma}{dt} = -E\dot{\gamma}_0 \exp\left(-\frac{t-t_0}{\hat{\tau}}\right) \quad (44)$$

In the case of hardening  $\sigma = \kappa_0 + H\gamma + \eta\dot{\gamma}$  until  $\dot{\gamma} = 0$ . Since  $\dot{\varepsilon} = 0$  we have  $\dot{\gamma}_\infty = 0$ , so  $\dot{\gamma}(t) = \dot{\gamma}_0 \exp[-(t-t_0)/\hat{\tau}]$  and  $\gamma = \gamma_0 + \hat{\tau}\dot{\gamma}_0 - \hat{\tau}\dot{\gamma}_0 \exp[-(t-t_0)/\hat{\tau}]$ . Then

$$\sigma = \kappa_0 + H(\gamma_0 + \hat{\tau}\dot{\gamma}_0 - \hat{\tau}\dot{\gamma}_0 \exp[-(t-t_0)/\hat{\tau}]) + \eta\dot{\gamma}_0 \exp\left(-\frac{t-t_0}{\hat{\tau}}\right) \quad (45)$$

and for  $t \rightarrow \infty$  we get  $\sigma = \kappa_0 + H(\gamma_0 + \hat{\tau}\dot{\gamma}_0)$ , as it should be expected from Eq. (2.4.1).

A similar process occurs if there is a reverse loading or unloading, as shown in Fig. 3d and in Fig. 3f in time. Consider a change from a positive (loading)  $\dot{\varepsilon} = \dot{\varepsilon}_l > 0$  to a negative (unloading) rate  $\varepsilon = \dot{\varepsilon}_u < 0$ . Then  $\dot{\gamma}_\infty(\dot{\varepsilon}_u) < 0$ . The stress is

$$\sigma = \underbrace{\kappa_0 + \eta\dot{\gamma}_\infty}_{< \kappa_0} + \underbrace{\eta(\dot{\gamma}_0 - \dot{\gamma}_\infty)}_{> 0} \underbrace{\exp\left(-\frac{t-t_0}{\hat{\tau}}\right)}_{1 \rightarrow 0} \quad (46)$$

The stress relaxes towards an horizontal asymptote at  $\kappa_0 + \eta\dot{\gamma}_\infty < \kappa_0$ , with a speed in time given by

$$\frac{d\sigma}{dt} = -E(\dot{\gamma}_0 - \dot{\gamma}_\infty) \exp\left(-\frac{t-t_0}{\hat{\tau}}\right) \quad (47)$$

This viscous relaxation takes place until the inviscid yield surface  $f_p = 0$  is crossed (i.e. when  $\sigma = \kappa_0$ ), which happens at time

$$t = t_0 - \hat{\tau} \log\left(\frac{\dot{\gamma}_\infty}{\dot{\gamma}_\infty - \dot{\gamma}_0}\right) \quad (48)$$

which obviously gives the limit  $t \rightarrow t_0 + \infty$  for  $\dot{\gamma}_\infty \rightarrow 0$ , corresponding to the relaxation case. After  $f_p = 0$  is crossed, the unloading continues elastically, see Fig. 3d. Note that even in the reverse loading case,  $\gamma$  continues to increase until the inviscid yield surface is crossed; i.e. as long as  $f_p > f = 0$ .

In Fig. 4 we show the behavior of the model under simple shear for different viscosities and a softening modulus, where the previous effects may be observed.

### 3. Incremental theory of $J_2$ -viscoplasticity with linear isotropic hardening

We develop an incremental solution for a step to build the computational implicit algorithm, first in this section with attention to the linear case. The solution of the step depends on whether the step is fully elastic (which solution is trivial), fully viscoplastic, or mixed elastic-to-viscoplastic or viscoplastic-to-elastic. We denote the time step by left-superindices as in  ${}^t(\bullet)$ , following the notation in e.g. [36, 1, 37].

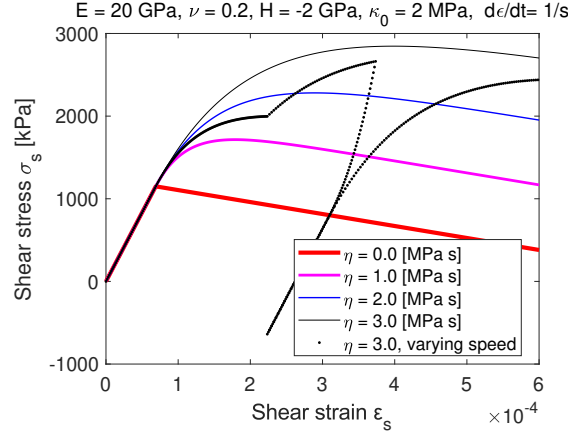


Figure 4: Influence of the loading rate or the viscosity parameter  $\eta$  on the predictions of the model.  $\eta = 0$  corresponds to the inviscid solution. Note that a change of loading rate has the same influence as a change of viscosity. Note also that the limiting elastoplastic tangent is reached in all cases, i.e.  $2\mu_{eq} = 2\mu H/(2\mu c^2 + H) = -1.45$  MPa, and that the stress offset in the asymptote is given by  $\eta_{s-eq}\dot{\epsilon}_s/c^2$ . Loading rate of continuous curves:  $\dot{\epsilon} = 1/s$ . Dotted curve has sharp changes in loading rates, being those of  $\dot{\epsilon}_s = 0.5/s, 1.0/s, -0.5/s, 1.0/s$ . Note that dissipative behaviour still takes place during reverse loading until the plastic yield function (elastic domain) is reached.

### 3.1. All the step is dissipative

In the typical predictor-corrector algorithms, the two components  ${}^{tr}\dot{\epsilon}_e$  and  ${}^{ct}\dot{\epsilon}_e$  are integrated in two successive sub-steps; indeed the  $-{}^{ct}\dot{\epsilon}_e$  is identified as  $\dot{\epsilon}_p$  in classical procedures, an identification which only holds at small strains [27] and which allows for the identification  $-\Delta{}^{ct}\epsilon_e \equiv \Delta\epsilon_p$ . The first of them (the trial part) is purely hyperelastic, conservative, i.e. during the step  ${}^{tr}\mathcal{D}^p = 0$ , but changes the stored energy from  ${}^t\Psi := \Psi({}^t\epsilon_e)$  to  ${}^{tr}\Psi := \Psi({}^{tr}\epsilon_e)$ . Then, the error in the fulfillment of the first principle during a step comes only from the dissipative part in a subsequent substep. Unfortunately, whereas this type of predictor-corrector algorithms are well-suited for elastoplasticity, in viscoplasticity the predictor phase cannot be easily isolated from the corrector phase because of the time-dependence (both effects occur simultaneously). This is manifest by the comparison of both Equations (26). The first one is independent of time so an increment may be applied to both hand sides and the result is independent of the time in which the increments took place, e.g.  $\Delta\gamma = \dot{\gamma}\Delta t$  and  $\Delta\epsilon = \dot{\epsilon}\Delta t$  so  $\Delta t$  cancels out. However, in the second one, time cannot be eliminated because the speed at which the increment takes place is important, since that speed changes the dissipated energy through the dashpot; for example in a quasi-static deformation the dashpot does not dissipate energy whatever the value of  $\eta$  is, but in a very fast process most dissipation comes from the dashpot. Noteworthy, Eq. (26)<sub>1</sub> is equivalent to establish  ${}^{t+\Delta t}f_p = 0$  integrated with a backward-Euler method (i.e. the solution from the radial return algorithm of Wilkins [38])

$$\Delta\gamma = \frac{1}{c} \frac{2\mu({}^{t+\Delta t}\hat{n} : \Delta\epsilon)}{2\mu + H/c^2} \equiv \frac{1}{c} \frac{2\mu({}^{tr}\hat{n} : \Delta\epsilon)}{2\mu + H/c^2} =: \Delta\gamma_\infty \quad (49)$$

Then, considering still the linear case with constant  $\kappa' = H$ ,  $g' = \eta$  and  $(\hat{\mathbf{n}} : \dot{\boldsymbol{\varepsilon}}) = (\hat{\mathbf{n}} : \Delta\boldsymbol{\varepsilon}) / \Delta t$  during the step (so  $\hat{\tau}$  and  $\dot{\gamma}_\infty$  are also constant), the *exact* integration of the equivalent viscoplastic strain is (i.e. no error is introduced if  $\hat{\mathbf{n}}$  is constant, which happens in proportional loading)

$$\begin{aligned}\Delta\gamma &= \int_t^{t+\Delta t} \dot{\gamma} dt = \int_t^{t+\Delta t} \left\{ \dot{\gamma}_\infty + [\dot{\gamma} - \dot{\gamma}_\infty] \exp\left(-\frac{\bar{t}-t}{\hat{\tau}}\right) \right\} d\bar{t} \\ &= \dot{\gamma}_\infty \Delta t + \hat{\tau} [\dot{\gamma} - {}^{t+\Delta t}\dot{\gamma}_\infty] \left[ 1 - \exp\left(-\frac{\Delta t}{\hat{\tau}}\right) \right] \neq 0\end{aligned}\quad (50)$$

with the definition given in Eq. (49) and the definition *during the current step* (i.e. from  $t$  to  $t+\Delta t$ ) of  ${}^{t+\Delta t}\dot{\gamma}_\infty \equiv {}^{tr}\dot{\gamma}_\infty \equiv \dot{\gamma}_\infty := \Delta\gamma_\infty / \Delta t$ . For small steps we have  $[(2\mu c^2 + H) / \eta] \Delta t =: \Delta t / \hat{\tau} \rightarrow 0$ , where the relaxation time in the present linear case is

$$\hat{\tau} = \frac{\eta}{2\mu c^2 + H} = \frac{\eta / c^2}{2\mu + H / c^2} \quad (51)$$

Note that the expected limits are recovered, e.g.  $\Delta t / \hat{\tau}$  small implies  $\Delta\gamma \simeq {}^t\dot{\gamma} \Delta t$  and for  $\Delta t / \hat{\tau} \rightarrow \infty$  we have  $\Delta\gamma \rightarrow \Delta\gamma_\infty + \hat{\tau} {}^t\dot{\gamma}$ . If  ${}^t\dot{\gamma} = 0$  we obtain  $\Delta\gamma = \dot{\gamma}_\infty [\Delta t - \hat{\tau} \xi(\Delta t)]$ . Consider Eq. (27) at  $t + \Delta t$  where the step has a uniform external strain speed given by  $\dot{\boldsymbol{\varepsilon}} = \Delta\boldsymbol{\varepsilon} / \Delta t$

$${}^{t+\Delta t}\dot{\gamma} = {}^{t+\Delta t}\dot{\gamma}_\infty + [\dot{\gamma} - {}^{t+\Delta t}\dot{\gamma}_\infty] \exp\left(-\frac{\Delta t}{\hat{\tau}}\right) \neq 0 \quad (52)$$

so

$$\Delta\dot{\gamma} := {}^{t+\Delta t}\dot{\gamma} - {}^t\dot{\gamma} = ({}^{t+\Delta t}\dot{\gamma}_\infty - {}^t\dot{\gamma}) \left[ 1 - \exp\left(-\frac{\Delta t}{\hat{\tau}}\right) \right] = {}^{tr}\dot{\gamma}_{neq} \xi(\Delta t) \quad (53)$$

where  ${}^{tr}\dot{\gamma}_{neq} := {}^{t+\Delta t}\dot{\gamma}_\infty - {}^t\dot{\gamma}$  is the trial non-equilibrated rate at  $t + \Delta t$ ; i.e. the difference between the “at infinite” (inviscid) rate during the step  $\Delta\gamma_\infty / \Delta t$  and the actual one at the beginning of the step  ${}^t\dot{\gamma}$ . The relaxation case is obtained when  $\dot{\boldsymbol{\varepsilon}} = \mathbf{0}$ , i.e.  $\Delta\boldsymbol{\varepsilon} = \mathbf{0}$ . Then  $\Delta\gamma_\infty = \dot{\gamma}_\infty = 0$  and  $\Delta\gamma = {}^t\dot{\gamma} \hat{\tau} \xi(\Delta t)$  and  $\Delta\dot{\gamma} = -{}^t\dot{\gamma} \xi(\Delta t)$ . In such case, the zero rate  $\dot{\gamma} = 0$  is obtained with  $\Delta\dot{\gamma} = -{}^t\dot{\gamma}$

$$-{}^t\dot{\gamma} = -{}^t\dot{\gamma} \left[ 1 - \exp\left(-\frac{\Delta t}{\hat{\tau}}\right) \right] \Rightarrow \frac{\Delta t}{\hat{\tau}} \rightarrow \infty \quad (54)$$

at time  $\Delta t \rightarrow \infty$ , where  $\Delta\gamma = {}^t\dot{\gamma} \hat{\tau}$ —c.f. again Eq. (2.4.1)

Consider the integration of the thermodynamical power balance (i.e. energy balance) during the step using the previous relations

$$\int_t^{t+\Delta t} {}^{tr}\dot{f} dt = \Delta f|_{D^p=0} := {}^{tr}f - {}^t f \quad (55)$$

$$\int_t^{t+\Delta t} {}^{ct}\dot{f} dt = -(2\mu c^2 + H) \Delta\gamma - \eta \Delta\dot{\gamma} \quad (56)$$



Noteworthy, if we require energy conservation, so during the step  $\Delta f = 0$  (as to obtain  ${}^{t+\Delta t}f = 0$  if  ${}^tf = 0$ ), we have

$$\begin{aligned} {}^{t+\Delta t}f - {}^tf &= \int_t^{t+\Delta t} {}^{tr}\dot{f}dt + \int_t^{t+\Delta t} {}^{ct}\dot{f}dt \\ &= ({}^{tr}f - {}^tf) - (2\mu c^2 + H) \Delta\gamma - \eta\Delta\dot{\gamma} = 0 \end{aligned} \quad (57)$$

so, using a backward Euler evaluation of the normal  ${}^{tr}f - {}^tf = 2\mu c ({}^{tr}\hat{\mathbf{n}} : \Delta\boldsymbol{\varepsilon})$ —this can be seen as the inverse of the relaxation case

$$\Delta\gamma = \frac{({}^{tr}f - {}^tf) - \eta\Delta\dot{\gamma}}{2\mu c^2 + H} = \frac{2\mu c ({}^{tr}\hat{\mathbf{n}} : \Delta\boldsymbol{\varepsilon})}{2\mu c^2 + H} - \frac{\eta\Delta\dot{\gamma}}{2\mu c^2 + H} \quad (58)$$

$$= \Delta\gamma_\infty - \hat{\tau}\Delta\dot{\gamma} \quad (59)$$

Using Eq. (53) into Eq. (58)

$$\begin{aligned} \Delta\gamma &= \frac{{}^{tr}f - {}^tf}{2\mu c^2 + H} - \frac{\eta}{2\mu c^2 + H} \left[ \frac{2\mu c ({}^{tr}\hat{\mathbf{n}} : \Delta\boldsymbol{\varepsilon}/\Delta t)}{2\mu c^2 + H} - {}^t\dot{\gamma} \right] \left[ 1 - \exp\left(-\frac{2\mu c^2 + H}{\eta}\Delta t\right) \right] \\ &= \underbrace{\Delta\gamma_\infty}_{\text{inviscid}} \underbrace{-\hat{\tau} {}^{tr}\dot{\gamma}_{neq} \left[ 1 - \exp\left(-\frac{\Delta t}{\hat{\tau}}\right) \right]}_{\text{viscous}} \end{aligned} \quad (60)$$

so we recover Eq. (50), but now from  ${}^{t+\Delta t}f = 0$  instead of from integrating directly  $\dot{\gamma}$ .

Summarizing, the solution for the linear viscoplastic problem is given by the system of equations given by Eqs. (53) and (50). Note that this solution recovers automatically those when  $\eta = 0$  (inviscid plasticity) and when  $\kappa = H = 0$  (viscoelasticity). Remarkably, the solutions of  $\Delta\gamma$  and  $\Delta\dot{\gamma}$  in Eqs. (53) and (50) are the *exact* solutions that fulfill, *during all the step*, the thermodynamic consistency given by  $f = 0$  from  $t$  to  $t + \Delta t$ , with the requirements that: (1) elasticity moduli  $\mu$ , hardening  $H$  and viscosity  $\eta$  are constant, and (2) the rate  $2\mu c(\hat{\mathbf{n}} : \dot{\boldsymbol{\varepsilon}})$  is constant during the step. In proportional loading in linear viscoplasticity, these are fulfilled. Figure 5 shows that the same solution is obtained for different time step increments. In other cases (nonlinear viscoelasticity or multiaxial non-proportional loading), the present solution is only an approximation, and backward-Euler evaluations are employed to recover the inviscid solution for  $\Delta t \rightarrow \infty$  or  $\eta = 0$ .

Once the values of  ${}^{t+\Delta t}\gamma$  and  ${}^{t+\Delta t}\dot{\gamma}$  are known, the elastic strain is computed from a backward-Euler scheme as

$${}^{t+\Delta t}\boldsymbol{\varepsilon}_e = \underbrace{{}^t\boldsymbol{\varepsilon}_e + \Delta\boldsymbol{\varepsilon}}_{{}^t\boldsymbol{\varepsilon}_e + \Delta{}^{tr}\boldsymbol{\varepsilon}_e} - \underbrace{\Delta\gamma c \, {}^{t+\Delta t}\hat{\mathbf{n}}}_{+\Delta{}^{ct}\boldsymbol{\varepsilon}_e} \quad (61)$$

and obviously from the hyperelastic relation with  $\mathbb{C}_e = d^2\Psi/d\boldsymbol{\varepsilon}_e \otimes d\boldsymbol{\varepsilon}_e$

$${}^{t+\Delta t}\boldsymbol{\sigma} = \mathbb{C}_e : {}^{t+\Delta t}\boldsymbol{\varepsilon}_e = K \text{tr}({}^{t+\Delta t}\boldsymbol{\varepsilon}_e) \mathbf{I} + 2\mu {}^{t+\Delta t}\boldsymbol{\varepsilon}_e^d \quad (62)$$

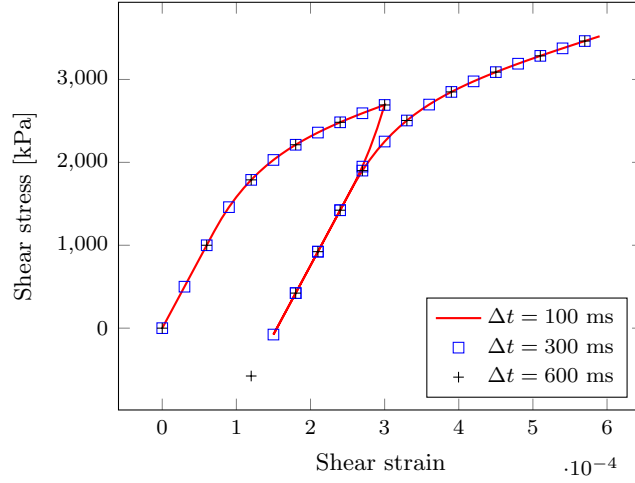


Figure 5: Loading-unloading-reloading with different time increments using the proposed algorithm. Note that viscoplastic solutions are coincident at specific computational points (step ends) regardless of the time-increment employed and of the lack of coincidence of step ends when crossing the yield surface or when loading is reversed.

Consequently, the consistent tangent modulus tensor during the step fully viscoplastic can be determined as

$${}^{t+\Delta t}\mathbb{C} = \frac{d {}^{t+\Delta t}\boldsymbol{\sigma}}{d {}^{t+\Delta t}\boldsymbol{\varepsilon}} = {}^{t+\Delta t}\mathbb{C}^v + {}^{t+\Delta t}\mathbb{C}^d = K\mathbf{I} \otimes \mathbf{I} + \frac{d {}^{t+\Delta t}\boldsymbol{\sigma}^d}{d {}^{t+\Delta t}\boldsymbol{\varepsilon}} \quad (63)$$

From  ${}^{t+\Delta t}\boldsymbol{\varepsilon}_e^d = {}^{tr}\boldsymbol{\varepsilon}_e^d - c\Delta\gamma {}^{t+\Delta t}\hat{\mathbf{n}}$ ,

$$\frac{d {}^{t+\Delta t}\boldsymbol{\varepsilon}_e^d}{d {}^{t+\Delta t}\boldsymbol{\varepsilon}} = \mathbb{P}^s - c\Delta\gamma \frac{d {}^{t+\Delta t}\hat{\mathbf{n}}}{d {}^{t+\Delta t}\boldsymbol{\varepsilon}} - c {}^{t+\Delta t}\hat{\mathbf{n}} \otimes \frac{d\Delta\gamma}{d {}^{t+\Delta t}\boldsymbol{\varepsilon}} \quad (64)$$

with—recall that  ${}^{t+\Delta t}\hat{\mathbf{n}} \equiv {}^{tr}\hat{\mathbf{n}} = {}^{tr}\boldsymbol{\sigma}^d / ||{}^{tr}\boldsymbol{\sigma}^d||$

$$\mathbb{N} := \frac{d {}^{t+\Delta t}\hat{\mathbf{n}}}{d {}^{t+\Delta t}\boldsymbol{\varepsilon}} = \frac{d {}^{tr}\hat{\mathbf{n}}}{d {}^{t+\Delta t}\boldsymbol{\varepsilon}} = \frac{2\mu}{||{}^{tr}\boldsymbol{\sigma}^d||} \left[ \mathbb{P}^s - {}^{tr}\hat{\mathbf{n}} \otimes {}^{t+\Delta t}\hat{\mathbf{n}} \right] \quad (65)$$

Using the conditions  ${}^{t+\Delta t}f = 0$  and  ${}^{t+\Delta t}\dot{\gamma}$  from Eq. (52), after some straightforward algebra, we arrive at

$${}^{t+\Delta t}\mathbb{C}^d := \frac{d {}^{t+\Delta t}\boldsymbol{\sigma}^d}{d {}^{t+\Delta t}\boldsymbol{\varepsilon}} = 2\mu \left[ 1 - \frac{2\mu}{2\mu + H/c^2} \left( 1 - \frac{\hat{\tau}}{\Delta t} \xi(\Delta t) \right) \right] \mathbb{K}^{-1} : \mathbb{P}^s \quad (66)$$

in which  $\mathbb{K}$  is

$$\mathbb{K} = \mathbb{I}^S + 2\mu c \hat{\tau} {}^{t\dot{\gamma}} \xi(\Delta t) \mathbb{N} \quad (67)$$

Of course, for this linear case, the tangent developed below for the nonlinear case may be equally used. Note that  $\mathbb{C}^d$  is also bounded by the deviatoric elastic tangent modulus

tensor  $\mathbb{C}_e^d$  and by the deviatoric consistent inviscid elastoplastic tangent modulus tensor  $\mathbb{C}_{ep}^d$  as shown in the continuum theory. In fact,

$$\mathbb{C}^d = \begin{cases} 2\mu\mathbb{P}^s \equiv \mathbb{C}_e^d & \text{for } \Delta t \rightarrow 0, \eta \rightarrow \infty \\ \frac{2\mu H/c^2}{2\mu + H/c^2} \mathbb{P}^s \equiv \mathbb{C}_{ep}^d & \text{for } \Delta t \rightarrow \infty, \eta \rightarrow 0 \end{cases} \quad (68)$$

### 3.2. Crossing the elastic domain limit

An important algorithmic issue is when a step is crossing the limit of the elastic domain, i.e. when it is initially elastic but ends being viscoplastic, or vice-versa (unloading). Assuming that time step  $t$  has no instantaneous viscoplastic flow (i.e. the previous step ended elastic), then  ${}^t\dot{\gamma} = 0$ . If  ${}^t\dot{\gamma} = 0$ , the step will be elastic unless  ${}^{tr}f \equiv {}^{tr}f_p > 0$ , because the condition  ${}^{t+\Delta t}f > 0$  is not possible. However, if  ${}^t f_p < 0$ , some part of the step is still elastic. In contrast to perfect plasticity, since speed affects the solution, the step must be partitioned to identify which part is dissipative if we want the exact solution for the linear proportional loading case. Indeed, the predictions in Fig. 5 have been obtained using these partitions. Then consider the following partition

$$\begin{cases} \Delta t = \text{total step} = \Delta t^c + \Delta t^* \\ \Delta t^c = \text{conservative part of the step} \\ \Delta t^* = \text{dissipative part of the step} \end{cases} \quad (69)$$

and apply the nomenclature to all variables, i.e.  $(\bullet)^c$  is for the conservative part of the step, and  $(\bullet)^*$  is for the dissipative part of the step. Recall that  $\Delta\epsilon/\Delta t$  is constant during all the step, so we can write

$$\frac{\Delta\gamma_\infty}{\Delta t} = \frac{2\mu c ({}^{tr}\hat{\mathbf{n}} : \Delta\epsilon/\Delta t)}{2\mu c^2 + H} = \frac{2\mu c ({}^{tr}\hat{\mathbf{n}} : \Delta\epsilon^*/\Delta t^*)}{2\mu c^2 + H} = \frac{\Delta\gamma_\infty^*}{\Delta t^*} = \frac{2\mu c ({}^{tr}\hat{\mathbf{n}} : \Delta\epsilon^c/\Delta t^c)}{2\mu c^2 + H} = \frac{\Delta\gamma_\infty^c}{\Delta t^c} \quad (70)$$

i.e.  $\dot{\gamma}_\infty = \dot{\gamma}_\infty^c = \dot{\gamma}_\infty^*$ . The first part of the step is given by  $\Delta t^c$  such that  ${}^{t+\Delta t^c}f = 0$ , but  ${}^\tau f < 0, \forall \tau \in (t, t + \Delta t^c)$ . The second sub-step, with  $\Delta t^*$  gives

$$\Delta\gamma^* \equiv \Delta\gamma = \dot{\gamma}_\infty \Delta t^* - \dot{\gamma}_\infty \hat{\tau} \xi(\Delta t^*) \quad (71)$$

and since  ${}^t\dot{\gamma} = {}^{t+\Delta t^c}\dot{\gamma} = 0$ , Eq. (53) gives

$${}^{t+\Delta t}\dot{\gamma} = \dot{\gamma}_\infty \xi(\Delta t^*) \quad (72)$$

where  $\Delta t^*$  is unknown, but can be obtained from  ${}^{t+\Delta t}f = 0$  with  ${}^{tr}\boldsymbol{\sigma} = d\Psi({}^{tr}\boldsymbol{\epsilon}_e)/d{}^{tr}\boldsymbol{\epsilon}_e$  i.e.

$${}^{t+\Delta t}f \equiv \overbrace{[c {}^{tr}\boldsymbol{\sigma} : {}^{tr}\hat{\mathbf{n}} - \kappa_0 - H {}^t\dot{\gamma}]}^{{}^{tr}f} - (2\mu c^2 + H) \Delta\gamma^* - \eta {}^{t+\Delta t}\dot{\gamma} = 0 \quad (73)$$

so

$${}^{t+\Delta t}f \equiv {}^{tr}f - (2\mu c^2 + H) [\dot{\gamma}_\infty \Delta t^* - \dot{\gamma}_\infty \hat{\tau} \xi(\Delta t^*)] - \eta \dot{\gamma}_\infty \xi(\Delta t^*) = 0 \quad (74)$$

Note that for the case  $\hat{\tau} = 0$  we have  $\xi(\Delta t^*) = [1 - \exp(-\Delta t^*/\hat{\tau})] = 0$  and

$${}^{t+\Delta t}f \equiv {}^{tr}f - (2\mu c^2 + H) \dot{\gamma}_\infty \Delta t^* = 0 \Rightarrow \Delta t^* = \frac{{}^{tr}f}{(2\mu c^2 + H) \dot{\gamma}_\infty} = \frac{{}^{tr}f}{2\mu c ({}^{tr}\hat{\mathbf{n}} : \Delta \boldsymbol{\varepsilon} / \Delta t)} \quad (75)$$

which gives the correct partition of the step in the computation of the dissipative part and conservative parts in inviscid elastoplasticity. In the more general case, Eq. (74) needs to be solved for numerically, e.g. using a Newton-Raphson scheme, with tangent

$$\frac{d^{t+\Delta t}f}{d\Delta t^*} = -2\mu c ({}^{tr}\hat{\mathbf{n}} : \Delta \boldsymbol{\varepsilon} / \Delta t) \{1 - \hat{\tau}[\xi(\Delta t^*) + \Delta t^* \xi'^*] - \eta \xi'^*\} \quad (76)$$

where  $\xi(\Delta t^*) = 1 - \exp(-\Delta t^*/\hat{\tau})$  and  $\xi'^* = -(1/\hat{\tau}) \exp(-\Delta t^*/\hat{\tau})$ . Note that the case  $\eta = \hat{\tau} = 0$  is automatically recovered by the first iteration in a Newton-Raphson method, e.g. it results in Eq. (75) if we depart from a first guess  ${}^{t+\Delta t}f^{[0]} = {}^{tr}f$ . Note also that if  $\Delta t^* = 0$ , then  $\xi(\Delta t^* = 0) = 0$  and  $\xi'^*(\Delta t^* = 0) = 1/\hat{\tau}$ , so

$$\frac{d^{t+\Delta t}f}{d\Delta t^*} = -2\mu c ({}^{tr}\hat{\mathbf{n}} : \Delta \boldsymbol{\varepsilon} / \Delta t) \{1 - 2\mu c^2 - H\} \quad (77)$$

which is the inviscid solution, because in such case  $\dot{\gamma} = 0$ .

### 3.3. Unloading case

In contrast to inviscid plasticity,  ${}^{tr}f_p < 0$  does not imply that the step ends up being elastic. As aforementioned, instead of the classical Kuhn-Tucker condition, the unloading case is detected by the computation of a resulting  ${}^{t+\Delta t}\dot{\gamma} < 0$  from a usual viscoplastic step, namely

$${}^{t+\Delta t}\dot{\gamma} = \underbrace{\dot{\gamma}_\infty}_{<0} + \underbrace{({}^t\dot{\gamma} - \dot{\gamma}_\infty)}_{>0} \exp\left(-\frac{\Delta t}{\hat{\tau}}\right) < 0 \quad (78)$$

Note that we may have  $\dot{\gamma}_\infty < 0$  but a final  ${}^{t+\Delta t}\dot{\gamma} < 0$  is not a possible solution. Note that after reversing loading,  ${}^t\dot{\gamma}_{neq} = \dot{\gamma}_\infty - {}^t\dot{\gamma} \not\leq 0$ , see Fig. 3f, where we seek to find the instant at  $C'$ . Then, for an accurate solution, we need to divide the step in a first sub-step  $\Delta t^*$  in which dissipation takes place and a second sub-step  $\Delta t^c$  in which no dissipation takes place. The size of the first sub-step is computed precisely from that condition using, for example, the residual

$$r_t := \Delta t^* - \hat{\tau}_0 \log\left(\frac{{}^*\dot{\gamma}_\infty - {}^t\dot{\gamma}}{{}^*\dot{\gamma}_\infty}\right) = 0 \quad \text{with } \Delta t^* \in (0, \Delta t) \quad (79)$$

where

$${}^*\dot{\gamma}_\infty = \frac{2\mu c ({}^*\hat{\mathbf{n}} : \Delta \boldsymbol{\varepsilon} / \Delta t)}{2\mu c^2 + H} < 0 \quad (80)$$

and  ${}^*\hat{\mathbf{n}} \neq {}^{tr}\hat{\mathbf{n}}$  is the normal when crossing the plastic yield surface  $f_p$ , i.e. when  ${}^{t+\Delta t}\dot{\gamma} \equiv {}^*\dot{\gamma} = 0$  (end of the viscoplastic substep and start of the elastic unloading)

$${}^*\hat{\mathbf{n}} = \frac{{}^*\boldsymbol{\sigma}^d(\Delta t^*)}{\|{}^*\boldsymbol{\sigma}^d(\Delta t^*)\|} \quad \text{with } {}^*\boldsymbol{\sigma}^d(\Delta t^*) = {}^t\boldsymbol{\sigma}^d + \frac{\Delta t^*}{\Delta t} 2\mu \Delta \boldsymbol{\varepsilon}^d \quad (81)$$

The scalar nonlinear Equation (79) is solved iteratively using any suitable method, e.g. a Newton-Raphson method, for which the tangent is

$$\frac{dr_t(\Delta t^*)}{d\Delta t^*} = 1 - \frac{{}^t\dot{\gamma} \hat{\tau}_0}{{}^*\dot{\gamma}_\infty ({}^*\dot{\gamma}_\infty - {}^t\dot{\gamma})} \frac{d{}^*\dot{\gamma}_\infty}{d\Delta t^*} \quad (82)$$

with

$$\frac{d{}^*\dot{\gamma}_\infty}{d\Delta t^*} = \frac{1}{\Delta t} \frac{2\mu c}{2\mu c^2 + H} \Delta \boldsymbol{\varepsilon} : \frac{d{}^*\hat{\mathbf{n}}}{d\Delta t^*} \quad (83)$$

and

$$\frac{d{}^*\hat{\mathbf{n}}}{d\Delta t^*} = \frac{2\mu}{\Delta t} \frac{1}{\|\boldsymbol{\sigma}^d(\Delta t^*)\|} (\mathbb{P}^s - {}^*\hat{\mathbf{n}} \otimes {}^*\hat{\mathbf{n}}) : \Delta \boldsymbol{\varepsilon}^d \quad (84)$$

The iterations are

$$[\Delta t^*]^{(j+1)} = [\Delta t^*]^{(j)} - \left[ \frac{dr^*(\Delta t^*)}{d\Delta t^*} \right]^{(j)-1} r^{*(j)} \quad (85)$$

and the first guess may be obtained using  $(\Delta t^*)^0 = 0$  and

$${}^*\dot{\gamma}_\infty^{(0)} := \frac{2\mu c ({}^t\hat{\mathbf{n}} : \Delta \boldsymbol{\varepsilon} / \Delta t)}{2\mu c^2 + H} \quad (86)$$

Thereafter

$$\Delta \gamma^* \equiv \Delta \gamma = \Delta^* \gamma_\infty + \hat{\tau} ({}^t\dot{\gamma} - {}^*\dot{\gamma}_\infty) \left[ 1 - \exp \left( -\frac{\Delta t^*}{\hat{\tau}} \right) \right] \quad (87)$$

Then, the remaining part of the sub-step  $\Delta t^c = \Delta t - \Delta t^*$  is elastic, with a deviatoric strain increment of

$$\Delta \boldsymbol{\varepsilon}^{dc} = \frac{\Delta t^c}{\Delta t} \Delta \boldsymbol{\varepsilon}^d \quad (88)$$

However, note that the elastic strains are computed from the trial ones directly as

$${}^{t+\Delta t} \boldsymbol{\varepsilon}_e = \underbrace{{}^t \boldsymbol{\varepsilon}_e + \Delta \boldsymbol{\varepsilon}}_{tr \boldsymbol{\varepsilon}_e} - \Delta \gamma^* {}^*\hat{\mathbf{n}} \quad (89)$$

### 3.4. Partitioned tangents

In the cases when the steps include sub-steps, we need a special, partitioned computation of the tangent. The partition of the step is

$$\Delta \boldsymbol{\varepsilon} = \Delta \boldsymbol{\varepsilon}^c + \Delta \boldsymbol{\varepsilon}^* = \frac{\Delta \boldsymbol{\varepsilon}}{\Delta t} \Delta t^c + \frac{\Delta \boldsymbol{\varepsilon}}{\Delta t} \Delta t^* \quad (90)$$

Then, if  $\mathbb{C}_{vp}(\Delta t^*)$  is the viscoplastic tangent for a step of size  $\Delta t^*$

$${}^{t+\Delta t} \mathbb{C} = \frac{d{}^{t+\Delta t} \boldsymbol{\sigma}}{d{}^{t+\Delta t} \boldsymbol{\varepsilon}} = \frac{d\Delta \boldsymbol{\sigma}}{d\Delta \boldsymbol{\varepsilon}} = \frac{d\Delta \boldsymbol{\sigma}}{d\Delta \boldsymbol{\varepsilon}^c} : \frac{d\Delta \boldsymbol{\varepsilon}^c}{d\Delta \boldsymbol{\varepsilon}} + \frac{d\Delta \boldsymbol{\sigma}}{d\Delta \boldsymbol{\varepsilon}^*} : \frac{d\Delta \boldsymbol{\varepsilon}^*}{d\Delta \boldsymbol{\varepsilon}} \quad (91)$$

$$= \mathbb{C}_e : \frac{d\Delta \boldsymbol{\varepsilon}^c}{d\Delta \boldsymbol{\varepsilon}} + \mathbb{C}_{vp}(\Delta t^*) : \frac{d\Delta \boldsymbol{\varepsilon}^*}{d\Delta \boldsymbol{\varepsilon}} \quad (92)$$

where, using Eq. (90)

$$\frac{d\Delta\epsilon^c}{d\Delta\epsilon} = \left. \frac{\partial\Delta\epsilon^c}{\partial\Delta\epsilon} \right|_{\Delta t^c=\text{const}} + \left. \frac{\partial\Delta\epsilon^c}{\partial\Delta t^c} \right|_{\Delta\epsilon=\text{const}} \otimes \frac{\partial\Delta t^c}{\partial\Delta\epsilon} = \frac{\Delta t^c}{\Delta t} \mathbb{I}^S + \frac{\Delta\epsilon}{\Delta t} \otimes \frac{\partial\Delta t^c}{\partial\Delta\epsilon} \quad (93)$$

and

$$\frac{d\Delta\epsilon^*}{d\Delta\epsilon} = \left. \frac{\partial\Delta\epsilon^*}{\partial\Delta\epsilon} \right|_{\Delta t^*=\text{const}} + \left. \frac{\partial\Delta\epsilon^*}{\partial\Delta t^*} \right|_{\Delta\epsilon=\text{const}} \otimes \frac{\partial\Delta t^*}{\partial\Delta\epsilon} = \frac{\Delta t^*}{\Delta t} \mathbb{I}^S + \frac{\Delta\epsilon}{\Delta t} \otimes \frac{\partial\Delta t^*}{\partial\Delta\epsilon} \quad (94)$$

where  $\partial\Delta t^c/\partial\Delta\epsilon$  and  $\partial\Delta t^*/\partial\Delta\epsilon$  are obtained from the respective conditions of  $f = 0$  and  $\dot{\gamma} = 0$  (depending on the condition governing the step partitioning), and once one condition is obtained, the other one is given by the complementarity of the other substep step; for example

$$\Delta t = \Delta t^c + \Delta t^* \Rightarrow \frac{\partial\Delta t}{\partial\Delta\epsilon} = \frac{\partial\Delta t^c}{\partial\Delta\epsilon} + \frac{\partial\Delta t^*}{\partial\Delta\epsilon} = \mathbf{0} \quad (95)$$

because  $\Delta t$  is constant, independent of  $\Delta\epsilon$ , so

$$\frac{\partial\Delta t^*}{\partial\Delta\epsilon} = -\frac{\partial\Delta t^c}{\partial\Delta\epsilon} \quad (96)$$

Here, we develop  $\partial\Delta t^*/\partial\Delta\epsilon$  for two cases: one starts initially elastic and ends being viscoplastic (see Sec. 3.2), other starts initially viscoplastic but ends being elastic (see Sec. 3.3).

#### 3.4.1. First case: crossing the elastic domain to the viscoplastic domain

In order to determine the  $\Delta t^*$ , we need to solve the nonlinear Eq. (74), which analytical closed-form solution is not easy to obtain, so a numerical one through the Newton-Raphson method is obtained. Once the solution is converged, Eq. (74) is fulfilled and  $\partial\Delta t^*/\partial\Delta\epsilon$  can be obtained by deriving Eq. (74) respect to  $\Delta\epsilon$ , which after some straightforward math gives

$$\frac{\partial\Delta t^*}{\partial\Delta\epsilon} = \frac{1}{\zeta} \frac{\partial {}^{tr}f}{\partial\Delta\epsilon} \quad (97)$$

with

$$\zeta = (2\mu c^2 + H)\dot{\gamma}_\infty \left\{ 1 - \hat{\tau} \left[ \xi(\Delta t^*) + \frac{\Delta t^*}{\hat{\tau}} \exp\left(-\frac{\Delta t^*}{\hat{\tau}}\right) \right] \right\} + \frac{\eta\dot{\gamma}_\infty}{\hat{\tau}} \exp\left(-\frac{\Delta t^*}{\hat{\tau}}\right) \quad (98)$$

and

$$\frac{\partial {}^{tr}f}{\partial\Delta\epsilon} = 2\mu c (\Delta\epsilon : \mathbb{P}_n : \mathbb{C}^e + {}^{tr}\hat{\mathbf{n}}) \quad (99)$$

#### 3.4.2. Second case: crossing the viscoplastic domain to the elastic domain

From the established relation in Eq. (79),

$$\frac{dr_t(\Delta\epsilon, \Delta t^*(\Delta\epsilon))}{d\Delta\epsilon} = \left. \frac{\partial r_t(\Delta t^*)}{\partial\Delta t^*} \right|_{\Delta\epsilon=\text{const}} \frac{\partial\Delta t^*}{\partial\Delta\epsilon} + \left. \frac{\partial r_t(\Delta t^*)}{\partial\Delta\epsilon} \right|_{\Delta t^*=\text{const}} = \mathbf{0} \quad (100)$$

so

$$\frac{\partial \Delta t^*}{\partial \Delta \epsilon} = - \left[ \frac{\partial r_t(\Delta t^*)}{\partial \Delta t^*} \right]_{\Delta \epsilon = \text{const}}^{-1} \frac{\partial r_t(\Delta t^*)}{\partial \Delta \epsilon} \Big|_{\Delta t^* = \text{const}} \quad (101)$$

where

$$\frac{\partial r_t(\Delta t^*)}{\partial \Delta \epsilon} \Big|_{\Delta t^* = \text{const}} = - \frac{{}^t \dot{\gamma} \hat{\tau}_0}{{}^* \dot{\gamma}_\infty ({}^* \dot{\gamma}_\infty - {}^t \dot{\gamma})} \frac{\partial {}^* \dot{\gamma}_\infty}{\partial \Delta \epsilon} \Big|_{\Delta t^* = \text{const}} \quad (102)$$

with

$$\frac{\partial {}^* \dot{\gamma}_\infty}{\partial \Delta \epsilon} \Big|_{\Delta t^* = \text{const}} = \frac{1}{\Delta t} \frac{2\mu c}{2\mu c^2 + H} {}^* \hat{\mathbf{n}} + \frac{1}{\Delta t} \frac{2\mu c}{2\mu c^2 + H} \Delta \epsilon : \frac{\partial {}^* \hat{\mathbf{n}}}{\partial \Delta \epsilon} \Big|_{\Delta t^* = \text{const}} \quad (103)$$

and

$$\frac{\partial {}^* \hat{\mathbf{n}}}{\partial \Delta \epsilon} \Big|_{\Delta t^* = \text{const}} = \frac{2\mu \Delta t^* / \Delta t}{\| {}^* \boldsymbol{\sigma}^d(\Delta t^*) \|} (\mathbb{P}^s - {}^* \hat{\mathbf{n}} \otimes {}^* \hat{\mathbf{n}}) \quad (104)$$

#### 4. Comparison with classical models

Frequently, different interpretations of the rheological model of Fig. 1 are considered as different models or formulations in the literature, even though in practice they may correspond to the same physics. However, equations are typically arranged in different ways so they become more convenient for specific purposes, allowing different interpretations and specially different algorithmic schemes, which are of most importance in finite element analysis.

##### 4.1. Perzyna formulation

The model from Perzyna [3], with different variations, is probably the best known model in computational viscoplasticity. The main asset of the model is the simplicity, because it does not require the fulfillment of the so-called consistency condition. The main handicap is the bad conditioning obtained as  $\eta \rightarrow 0$ , because the model is given by simply stating the rate as  $\dot{\gamma} = \langle f_p \rangle / \eta$ , where  $f_p$  is the plasticity yield function (i.e.  $f$  for  $\eta = 0$ ) and  $\langle \bullet \rangle$  is the Macaulay bracket. Hence, the inviscid solution cannot be recovered. A possible time integration algorithm may be simply obtained by the formulae  ${}^{t+\Delta t} \dot{\gamma} = \langle {}^{tr} f_p \rangle / \eta$  and  $\Delta \gamma = {}^t \gamma + {}^{t+\Delta t} \dot{\gamma} \Delta t$ . Perzyna's model is also frequently written using a dimensionless viscosity parameter  $\bar{\eta}$ , an exponent  $N \equiv 1/\epsilon \geq 1$ , and a nondimensional inviscid yield function  $f_p / \bar{\kappa}$ , with  $\bar{\kappa}$  being the nondimensionalization factor. This is the so-called power model

$$\dot{\gamma} = \frac{\langle \phi(f_p) \rangle}{\bar{\eta}} \text{ with } \phi(f_p) := \left( \frac{f_p}{\bar{\kappa}} \right)^N \quad (105)$$

which is also undefined for  $\bar{\eta} = 0$  (hence the source of numerical problems in some implementations). For simplicity in the comparison we use the (constant, initial) value  $\bar{\kappa} = {}^0 \kappa$  (this factor is included only in some formulations). In this case Eq. (105) may be re-written as

$$f := f_p - \bar{\kappa} \bar{\eta}^{1/N} \dot{\gamma}^{1/N} = 0 \quad (106)$$

i.e. we can write the energy conservation principle as

$$f := f_p - g(\dot{\gamma}) = 0 \text{ with } g(\dot{\gamma}) = \bar{\kappa} \bar{\eta}^{1/N} \dot{\gamma}^{1/N} = \bar{\kappa} \bar{\eta}^\epsilon \dot{\gamma}^\epsilon \quad (107)$$

so we recover our formulation as given in Eq. (17), and where the instantaneous viscosity modulus of our formulation is

$${}^t\eta = g' = \frac{d^t g}{d^t \dot{\gamma}} = \frac{1}{N} \bar{\kappa} \bar{\eta}^{1/N} \dot{\gamma}^{(1/N-1)} = \epsilon \bar{\kappa} \bar{\eta}^\epsilon \dot{\gamma}^{\epsilon-1} \quad (108)$$

For the linear case with  $N = \epsilon = 1$

$$\dot{\gamma} = \frac{f_p}{\eta} \quad \text{so} \quad g(\dot{\gamma}) = \eta \dot{\gamma} \quad \text{and} \quad g' \equiv \eta = \bar{\kappa} \bar{\eta} \quad (109)$$

An issue highlighted by Peric [39], is that when  $\epsilon \rightarrow 0$  for which one would assume to recover an inviscid limit, the stress approaches the limit  $2\bar{\kappa}$ . This is apparent particularizing Eq. (106) for this case, which brings  $f(\epsilon \rightarrow 0) \rightarrow f_p - \bar{\kappa} = 0$  instead of  $f_p = 0$ . However, for the also inviscid limit  $\bar{\eta} \rightarrow 0$  the correct  $f_p = 0$  is obtained. A different proposal, given in [39, 21] (and therein references) and in [19], to overcome the inconsistency in the sensitivity parameter  $\epsilon$ , is

$$\dot{\gamma} = \frac{\langle \bar{\phi}(f_p) - 1 \rangle}{\tilde{\eta}} \quad \text{with} \quad \bar{\phi}(f_p) := \left( \frac{f_p}{\bar{\kappa}} + 1 \right)^{\tilde{N}} \quad (110)$$

where  $\bar{\kappa}$  plays again the role of yield stress. In this case, following the rehological model, we have

$$f := f_p - g(\dot{\gamma}) = f_p - \underbrace{\bar{\kappa}[(\dot{\gamma} \tilde{\eta} + 1)^{1/\tilde{N}} - 1]}_{g(\dot{\gamma})} = 0 \quad (111)$$

which, note, recovers the inviscid limit for the cases  $\dot{\gamma} = 0$ ,  $\tilde{\eta} = 0$  and  $1/\tilde{N} = 0$ , hence the preference for this model in the computational mechanics literature. In the linear case, we have the same solution as the Perzyna model, i.e.  $\tilde{\eta} = \bar{\eta} = \eta/\bar{\kappa}$  and  $\tilde{N} = N = \epsilon = 1$ .

In summary, the Perzyna-type models are just a particular case of our formulation, but our algorithmic solution is well conditioned regardless of the value of the viscosity  $\eta$  (or  $\bar{\eta}$ ). Finally, we note that the common setting in the materials science literature does not normalize the yield function nor the viscosity parameter, so they have dimensions of stress.

#### 4.2. Duvaut-Lions formulation

Another frequently used formulation in viscoplasticity is the Duvaut-Lions formulation. Motivated on that framework, other models have also been presented, see e.g. [39]. The algorithmic advantage of the Duvaut-Lions model respect to the Perzyna formulation is that the inviscid case is automatically recovered because, in fact, the viscous solution is computed as a regularization of the inviscid one, which is computed first. The model is frequently presented as (see e.g. Eq. (2.7.13) in [20], adapted herein to our notation; for example the tensorial  $\dot{\gamma}$  in [20] is  $c\dot{\gamma}$  here because our  $\dot{\gamma}$  is the uniaxial equivalent, and  $f$  in [20] is our  $f_p/c$ )

$$c\dot{\gamma} = \frac{1}{2\mu\bar{\tau}} \hat{\mathbf{n}} : \left( \boldsymbol{\sigma}^d - \frac{t_\kappa}{c} \hat{\mathbf{n}} \right) \quad \text{if } f_p > 0; \quad \dot{\gamma} = 0 \quad \text{otherwise} \quad (112)$$

Recall that  $\hat{\mathbf{n}} = \boldsymbol{\sigma}^d / \|\boldsymbol{\sigma}^d\|$  and  $\bar{\tau}$  is a relaxation time. Note that in Eq. (112)  $\boldsymbol{\sigma}$  is the stress, which may be outside the inviscid yield surface, and since  $\boldsymbol{\sigma}^d$  has the direction  $\hat{\mathbf{n}}$ , and  $t_\kappa$  is



the inviscid uniaxial yield stress,  ${}^t\kappa/c \hat{\mathbf{n}}$  is the projection of the stress onto the inviscid yield surface. This equation may be written as

$$2\mu\bar{\tau}c^2\dot{\gamma} = f_p \iff \dot{\gamma} = \frac{f_p}{2\mu c^2\bar{\tau}} \left( = \frac{f_p}{\eta}, \text{ as seen below} \right) \quad (113)$$

or

$$f := f_p - 2\mu c^2\bar{\tau}\dot{\gamma} = 0 \quad (114)$$

so

$$f := f_p - g(\dot{\gamma}) = 0 \quad \text{with } g(\dot{\gamma}) = 2\mu c^2\bar{\tau}\dot{\gamma} = c^2\tilde{\eta}\dot{\gamma} = \eta\dot{\gamma} \quad (115)$$

with  $\bar{\tau} = \tilde{\eta}/2\mu = \eta/2\mu c^2$  (c.f. Eq. (2.7.12) in Simo & Hughes [20], and note that  $\bar{\tau} \neq \hat{\tau}$  and  $\tilde{\eta} \neq \eta$ ). The relation between both characteristic relaxation times is given by the term  $\eta\dot{\gamma}$ , as

$$\bar{\tau} = \frac{(2\mu + H/c^2)\hat{\tau}}{2\mu} \quad (116)$$

which differ for the hardening case. Remarkably, with this identification, Eqs. (105) and (112) are identical for  $N = 1$ , so are the models, which are also a particular case of our continuum formulation.

However, the difference between both Perzyna and Duvaut-Lions models often refer to the ideas behind the algorithmic setting. Indeed, the immediate implementation of Eq. (109) is, integrating the expression during the step considering the trial overstress:

$$(a) \text{ Trial step: } \gamma \text{ frozen and } f_p \rightarrow {}^{tr}f_p; (b) \text{ Corrector step: } \Delta\gamma = \frac{{}^{tr}f_p}{\eta}\Delta t \quad (117)$$

which gives immediately the increment in the equivalent viscoplastic strain  $\gamma$  upon knowledge of the trial inviscid plastic yield function  ${}^{tr}f_p$ , which is computed in the first “predictor” sub-step keeping frozen  $\gamma$  as in inviscid plasticity (recall that we argued that this partition is not consistent in the viscoplasticity case). Of course, at the end of the step  ${}^{t+\Delta t}f_p \neq 0$ . As long as  $f_p > 0$ , the step is viscoplastic. Equation (117) is very simple and attractive, but is ill-conditioned for  $\eta \rightarrow 0$ , so the inviscid case is not recovered by the algorithm, and numerical difficulties have been reported [39, 20, 21], etc.

On the contrary, the approach given by Eq. (112) considering a relaxation of the inviscid yield function, motivates a different implementation, taking the constant rate  $\dot{\gamma} = \Delta\gamma/\Delta t$

$$\underbrace{2\mu c^2\bar{\tau}}_{\eta} \frac{\Delta\gamma}{\Delta t} = \underbrace{\frac{{}^t f_p + \Delta {}^{tr} f_p}{{}^{tr} f_p}}_{\substack{{}^{tr} f_p \\ {}^{t+\Delta t} f_p}} \underbrace{\frac{\Delta {}^{ct} f_p}{-2\mu\Delta\gamma - H\Delta\gamma}}_{\Delta {}^{ct} f_p} \quad (118)$$

so factoring-out  $\Delta\gamma$  —c.f. Eq. (3.7.5) in Simo and Hughes [20] and recall the conversions explained before Eq. (112)

$$c\Delta\gamma = \frac{{}^{tr}f_p/2\mu c}{\frac{\bar{\tau}}{\Delta t} + 1 + H/2\mu c^2} \quad (119)$$

In contrast with the implementation in Eq. (117), this form is well conditioned for  $\eta \rightarrow 0$  and  $\bar{\tau} \rightarrow 0$ , cases in which the inviscid solution is recovered. However, note that Eq. (119) is valid only for the specific Eqs. (112) or (109), but not for the more general case, often more descriptive of experimental results, of Eq. (105) (the reason why the implementation of Eq. (117) is preferred in most works in the literature), and even in the linear proportional case, it does not bring the exact solution. Interestingly, note that the actual difference between the Perzyna and the Duvaut-Lions model is just about the integration of the corrector contribution and the related computational algorithm, not about any physical consideration, so they are indeed the same “model”. Namely, Eqs. (117) and Eq. (118) just differ in the implicit consideration of the inviscid terms in Eq. (118), which are neglected in the integration in Eq. (117). This is the reason behind its ill-conditioning when  $\eta = 0$ , when the inviscid terms become the only dissipative contribution in the step.

#### 4.3. Consistency model

Another model developed to solve the previous issues is the so-called “consistency” model [22, 24, 25]. In this model, using a formulation simplified to the case at hand to facilitate comparisons, a viscoplastic yield condition is assumed  $f_{vp}(\boldsymbol{\sigma}, \gamma, v)$ , where  $\gamma$  is the consistency parameter and  $v$  is another variable, representing in many cases  $\dot{\gamma}$ . Consider the present case—c.f. Eq. (17)

$$f_{vp} := c \, \hat{\mathbf{n}} : \boldsymbol{\sigma} - \kappa(\gamma) - g(v) \quad (120)$$

e.g. using the linear relations  $\kappa(\gamma) = \kappa_0 + H\gamma$  and  $g(v) = \eta v$

$$f_{vp} := c \, \hat{\mathbf{n}} : \boldsymbol{\sigma} - \kappa_0 - H\gamma - \eta v \quad (121)$$

The viscoplastic yield function  $f_{vp}$  governs the loading/unloading criteria as if it were a classical yield function in elastoplasticity, i.e. follow the Kuhn-Tucker loading/unloading conditions

$$f_{vp} \leq 0, \dot{\gamma} > 0 \text{ and } \dot{\gamma} f_{vp} = 0 \quad (122)$$

and  $f_{vp} < 0$  implies purely elastic behavior, regardless of the value of  $\dot{\gamma}$ , see Sec. 2.2 in Heeres et al [25]. Indeed, it is required that during loading  $\dot{\gamma} = v$ , and upon unloading ( $f_{vp} < 0$ ), then  $\gamma$  remains constant. However, after unloading, during the unloading and reloading process, the value of  $v = \dot{\gamma}_u$  (subscript standing for onset of unloading) is frozen, so after the first unloading, the elastic domain is enlarged by  $\eta v \equiv \eta \dot{\gamma}_u$ , so thereafter during elastic behavior  $v \neq 0$  whereas  $\dot{\gamma} = 0$ , being this the reason why the consistency model needs  $v$  and  $\dot{\gamma}$  (they may take different values). Remarkably, this is the main theoretical (practical) difference between our present proposal and the consistency model. We emphasize that we did not make the assumption of the existence of a yield viscoplastic surface  $f_{vp}$ . Our function  $f = 0$  is just a power balance which guarantees the fulfillment of the first principle of thermodynamics. Then, our loading/unloading condition is simply given by the value of  $\dot{\gamma}$ . As long as  $\dot{\gamma} > 0$ , viscoplastic flow takes place; the absence of it (elastic loading) requires  $\dot{\gamma} = 0$ , and we do not need the additional variable  $v$ . As a consequence, our model behaves as the Perzyna model, whereas the consistency model reloads to the previous unloading stress-strain point, as noted in Heeres et al [25], see therein Figures 1 and 3. Also noteworthy, the Perzyna and

the consistency models give the same results if no unloading takes place, see Figs. 4 and 6 in Heeres et al [25]. We mention that the inclusion of the possibility of using  $\eta \rightarrow 0$  with more general viscoplastic constitutive equations of the type Eq. (105) comes with the cost of a more complex algorithm, e.g. Sec. 4.2 in Heeres et al [25].

#### 4.4. Models without yield function. Nonlinear viscoelasticity

Many models, as the Norton-Odqvist law, do not employ a yield function (i.e. a yield stress). This implies that the viscoplastic strain is given directly in terms of the stress, e.g. Norton's law is

$$\dot{\gamma} = \left( \frac{c \|\boldsymbol{\sigma}^d\|}{\check{\eta}} \right)^N \quad (123)$$

with  $\|\boldsymbol{\sigma}^d\| \equiv \hat{\mathbf{n}} : \boldsymbol{\sigma}$  and

$$-{}^{ct}\dot{\boldsymbol{\epsilon}}_e = c\dot{\gamma}\hat{\mathbf{n}} \quad (124)$$

Norton's law can be written, taking  $\kappa(\gamma) = 0$ , as

$$f \equiv f_p - g(\dot{\gamma}) \equiv c\hat{\mathbf{n}} : \boldsymbol{\sigma} - \check{\eta}\dot{\gamma}^{1/N} = 0 \quad (125)$$

Then, if we just take  $f_p = c\hat{\mathbf{n}} : \boldsymbol{\sigma}$  and  $g(\dot{\gamma}) = \check{\eta}\dot{\gamma}^{1/N}$ , and  $g'(\dot{\gamma}) = \frac{1}{N}\check{\eta}\dot{\gamma}^{1/N-1}$ , our formulation and integration algorithm are unchanged and well-conditioned, being this just a particular case. Indeed, the absence of yield stress is the case of viscoelasticity, so the present formulation recovers naturally the viscoelasticity formulation as a particular case; see e.g. [34, 33]. Note that all equations are valid just setting  $\kappa(\gamma) = 0$ , e.g. Eqs. (23), (26) and (27), and that the evolution equation in Refs. [34, 33] is, for the linear isotropic case considered therein

$$-{}^{ct}\dot{\boldsymbol{\epsilon}}_e = c^2\eta^{-1}\boldsymbol{\sigma}^d \quad (126)$$

which is just a reformatting of Eqs. (123) and (124).

#### 4.5. Models with kinematic hardening

The friction element in the rheological model has only isotropic hardening. However, the formulation is essentially valid for kinematic hardening, including the nonlinear kinematic hardening case (e.g. Ohno-Wang model). To this end, it only suffices to include a spring in parallel to the Bingham model, and include in the formulation the corresponding stored energy (note that kinematic hardening has energetic nature). This setting also holds in the case of large strains employing the Kröner-Lee multiplicative decomposition. For more details on this type of formulation see Refs. [27, 28, 29, 31, 30]

### 5. Uniaxial numerical comparisons with classical models for linear viscoplasticity

In this section we compare the results against other formulations (models and algorithms). We consider in this case the homogeneous, proportional linear case under loading and reverse loading to highlight similarities and differences, as often performed in the literature. A single integration point is subjected to an infinitesimal shear load with a constant shear strain

rate. For this comparison, the proposed model and other three well-known models (Perzyna, Duvault-Lions and consistency model) are implemented. Different values of shear strain rate and different values of the time increment are also applied in order to analyze the influence on the viscoplastic response and on the accuracy. The constitutive material parameters are given in Table 1. For the other models, the proper equivalence, presented in the previous sections, are employed.

Table 1: Constitutive parameters for the viscoplastic model

$E$ [kPa]	$\nu$	$\eta$ [kPa s]	$\kappa_0$ [kPa]	$H$ [kPa]
$2.0E07$	0.2	$2.0E03$	$2.0E03$	$5.0E06$

Figures 6 and 7 show the comparison including stress reversals for different shear strain rate and different time increments. The stress reversals consist of an initial loading phase (up to a shear strain of  $3.0 \times 10^{-4}$ ), then an unloading phase is applied until shear strain of  $1.5 \times 10^{-4}$ , and finally a reloading phase is followed to a shear strain of  $6.0 \times 10^{-4}$ . It can be observed that the significant difference in the viscoplastic behavior of different models starts from the moment of crossing the limit of the elastic domain at  $\kappa_0/\sqrt{3} = 1,154.7$  kPa. A noticeable difference can be seen during the unloading phase. Our proposed consistency viscoplasticity model uses the viscoplastic multiplier rate ( $\dot{\gamma}$ ) to check whether dissipation occurs. Therefore, dissipation, and hence viscoplastic deformation, is produced as long as  $\dot{\gamma} > 0$ . Our model unloads elastically when  $\dot{\gamma}$  just vanishes. This behavior is similar to that of both the Perzyna model and the Duvaut-Lions model due to the effect known as “overstress”. On the contrary, the consistency model [22, 24, 25] always unloads elastically because the dynamic loading surface is treated as a yield surface, enclosing an elastic domain. This different unloading behavior also leads to a noticeable difference in the subsequent reloading phase.

Also noticeable is that the Perzyna and Duvaut-Lions models related integration algorithms give results close to those of our model for small strain rates, when an accurate integration of the rate  $\dot{\gamma}$  (and hence of the dynamic contribution) is not so relevant (e.g. the case for  $|\dot{\epsilon}_{xy}| = 0.5/s$ ); in the loading phase a similar result is also observed with the consistency model in [22, 24, 25]. However, as strain rate increases and the dynamic contribution becomes more relevant, the difference between models is more noticeable. Indeed, unlike other models, since our model gives the exact solution for this linear case, the strain rate *does not* affect the accuracy of our predictions, and in turn, this accuracy is not affected by the time increment of the step.

Another relevant difference is observed for the consistency model, which is apparent specially in Fig. 6a. During the reloading phase, the trial value of  $f_{vp}$  governs the instant when the step becomes fully viscoplastic (even if there is an initial fraction which would be elastic). Then, because of this numerical inaccuracy, it regains viscoplastic behavior before reaching the previous unloading stress point. Of course for small steps, this effect becomes negligible, see Figs. 6b and 7.

The relaxation behavior of all models is also analysed. To this end, the shear strain is increased employing a constant shear strain rate  $\dot{\epsilon}_{xy} = 1.0/s$  to achieve a maximum shear strain of  $3.0 \times 10^{-4}$ , and thereafter is left constant. Figure 8 shows the results of this simulation

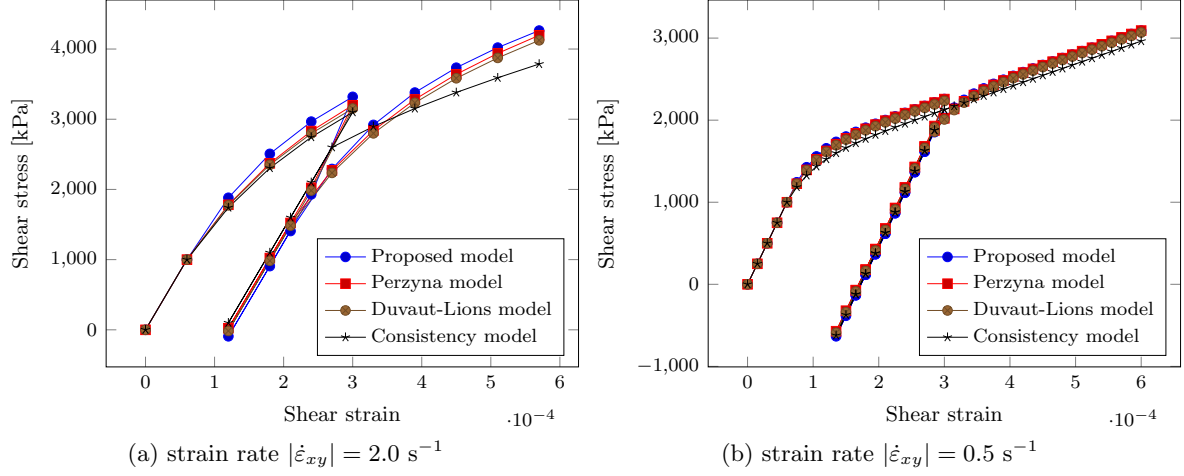


Figure 6: Loading-unloading-reloading with different models for  $\Delta t = 3.0 \times 10^{-5}$  s

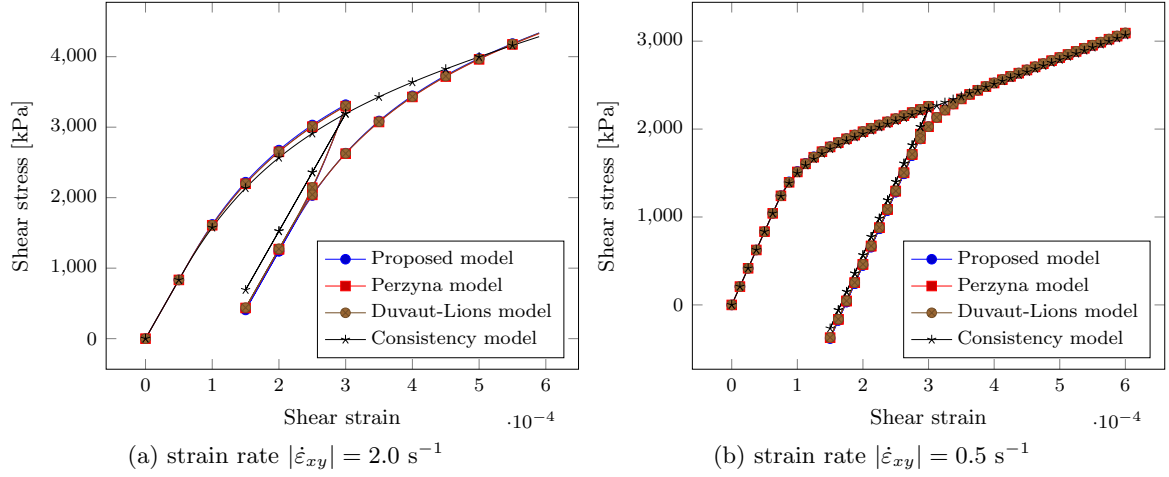


Figure 7: Loading-unloading-reloading with different models for  $\Delta t = 5.0 \times 10^{-6}$  s

for different time increments. Again, for small step sizes, the Perzyna model shows the same response as our proposed model.

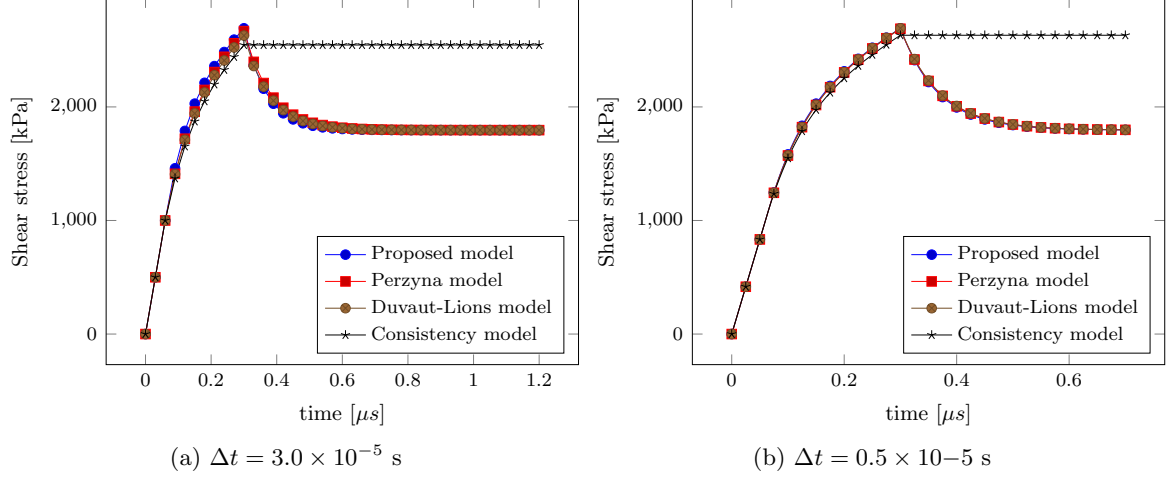


Figure 8: Relaxation: shear stress decay at constant strain with different models

Furthermore, in order to check the accurate performance of our proposed consistency viscoplasticity model we have performed a numerical testing for the case of  $\eta = 0.0$ , i.e. totally elasto-plastic model. Figure 9 represents a comparison of results obtained by different models. To avoid the ill-conditioning of the Perzyna model for  $\eta \rightarrow 0$ , a small  $\eta$  and quadruple (real\*64 type) precision has been employed. It can be seen that all models give the same solution for zero viscosity, except for the consistency model. Again, this difference is due to the use of the trial  $f_{vp}$  value to detect a viscoplastic step and consider it fully viscoplastic (note that the initial error is just maintained during the rest of the simulation, and vanishes when using small  $\Delta t$ ).

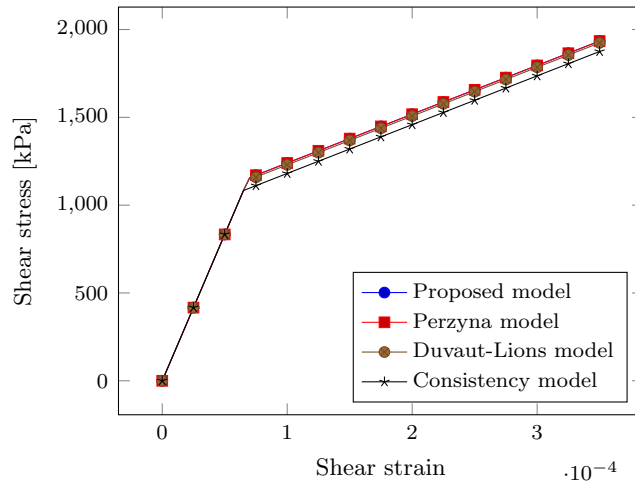


Figure 9: Shear stress - strain curves for viscosity  $\eta = 0$

## 6. General discrete formulation: A simple backward-Euler integration algorithm for non-constant material parameters

In this section we introduce a general formulation for the nonlinear viscoelasticity case, which obviously recovers the aforesaid linear formulation as a particular case.

### 6.1. Local Newton algorithm for the fully viscous step

We have shown in the previous examples that the linear model is capable of recovering the exact solution in the proportional case. In most practical loading cases at a stress point in a finite element simulation, the loading in a step is almost proportional (meaning that the change in the direction of  $\hat{\mathbf{n}}$  is small). Then, it seems reasonable to develop an integration algorithm that recovers that exact solution for the linear proportional case. To this end, in contrast with typical viscoplasticity algorithms, two independent variables are considered at each step, namely  ${}^t\gamma$  and  ${}^t\dot{\gamma}$ . Two conditions are enforced for the integration algorithm. The first one is the preservation of energy for  $\dot{\gamma} \neq 0$ ; i.e. Eq. (16)<sub>1</sub> if  ${}^{t+\Delta t}\dot{\gamma} \neq 0$

$${}^{t+\Delta t}r_f({}^{t+\Delta t}\gamma, {}^{t+\Delta t}\dot{\gamma}) = c {}^{t+\Delta t}\boldsymbol{\sigma} : {}^{t+\Delta t}\hat{\mathbf{n}} - \kappa ({}^{t+\Delta t}\gamma) - g({}^{t+\Delta t}\dot{\gamma}) \quad (127)$$

$$= \underbrace{c {}^{tr}\boldsymbol{\sigma} : {}^{tr}\hat{\mathbf{n}} - {}^t\kappa - {}^tg - c^2\Delta\gamma \mathbb{C}_e : {}^{tr}\hat{\mathbf{n}} - \Delta\kappa - \Delta g}_{\Delta^{ct}f} \rightarrow 0 \quad (128)$$

with  $\Delta(\cdot) = {}^{t+\Delta t}(\cdot) - {}^t(\cdot)$  and note that as in perfect plasticity,  ${}^{t+\Delta t}\hat{\mathbf{n}} = {}^{tr}\hat{\mathbf{n}} = {}^{tr}\boldsymbol{\sigma}^d / \| {}^{tr}\boldsymbol{\sigma}^d \|$ . The second one gives the relation for the conservation during the step, which relates  $\gamma$  and  $\dot{\gamma}$  through the solution of the corresponding differential Equation (24), starting at  $\gamma_0 = {}^t\gamma$  and ending at  $\gamma = {}^{t+\Delta t}\gamma$ , with a constant  $\dot{\epsilon} = \Delta\epsilon / \Delta t$  during the step—c.f. Eq. (53)

$${}^{t+\Delta t}r_{\dot{\gamma}}({}^{t+\Delta t}\gamma, {}^{t+\Delta t}\dot{\gamma}) := {}^{t+\Delta t}\dot{\gamma} - {}^{t+\Delta t}\dot{\gamma}_{\infty} - [{}^t\dot{\gamma} - {}^{t+\Delta t}\dot{\gamma}_{\infty}] \exp\left(-\frac{\Delta t}{t+\Delta t\hat{\tau}}\right) \rightarrow 0 \quad (129)$$

In the previous expressions

$$\left\{ \begin{array}{l} {}^{t+\Delta t}\hat{\tau}({}^{t+\Delta t}\dot{\gamma}, {}^{t+\Delta t}\gamma) := g'({}^{t+\Delta t}\dot{\gamma}) / {}^{t+\Delta t}h({}^{t+\Delta t}\gamma) \\ {}^{t+\Delta t}\dot{\gamma}_{\infty}(\Delta\epsilon, {}^{t+\Delta t}\gamma) := [c {}^{t+\Delta t}\hat{\mathbf{n}} : \mathbb{C}_e : \Delta\epsilon / \Delta t] / {}^{t+\Delta t}h({}^{t+\Delta t}\gamma) \\ {}^{t+\Delta t}h({}^{t+\Delta t}\gamma) := c^2 {}^{t+\Delta t}\hat{\mathbf{n}} : \mathbb{C}_e : {}^{t+\Delta t}\hat{\mathbf{n}} + \kappa'({}^{t+\Delta t}\gamma) \\ {}^{t+\Delta t}\boldsymbol{\sigma}({}^{t+\Delta t}\epsilon_e(\Delta\epsilon, {}^{t+\Delta t}\gamma)) = \mathbb{C}_e : {}^{t+\Delta t}\epsilon_e(\Delta\epsilon, {}^{t+\Delta t}\gamma, {}^{t+\Delta t}\dot{\gamma}) \\ {}^{t+\Delta t}\hat{\mathbf{n}}(\Delta\epsilon) = {}^{t+\Delta t}\boldsymbol{\sigma}^d / \| {}^{t+\Delta t}\boldsymbol{\sigma}^d \| = {}^{tr}\boldsymbol{\sigma}^d(\Delta\epsilon) / \| {}^{tr}\boldsymbol{\sigma}^d(\Delta\epsilon) \| \end{array} \right. \quad (130)$$

where we declared explicitly the dependencies for further reference and note that  ${}^{t+\Delta t}\hat{\mathbf{n}} : \mathbb{C}_e : {}^{t+\Delta t}\hat{\mathbf{n}} = 2\mu$  (constant). The two residues can be written in vector form as

$$\mathbf{R}(\mathbf{E}) = \begin{Bmatrix} r_{\dot{\gamma}} \\ r_f \end{Bmatrix} \rightarrow \mathbf{0} \quad \text{with} \quad \mathbf{E} = \begin{Bmatrix} {}^{t+\Delta t}\dot{\gamma} \\ {}^{t+\Delta t}\gamma \end{Bmatrix} \quad (131)$$

The residual vector equation is solved using the Newton-Raphson method, where the solution is updated at iteration  $(j + 1)$  from the known values at iteration  $(j)$  by

$$\mathbf{E}^{(j+1)} = \mathbf{E}^{(j)} - [\nabla \mathbf{R}^{(j)}]^{-1} \mathbf{R}^{(j)} \quad (132)$$

until

$$\|\mathbf{R}^{(j+1)}\| \leq tol \quad (133)$$

where  $(\bullet)^{[j]}$  indicates quantities for iteration  $[j]$  at time step  $t + \Delta t$ . For the first iteration, we take  $\mathbf{E}_i^{[0]} = [\dot{\gamma}, \gamma]^T$  and the trial value  ${}^{tr}\boldsymbol{\sigma} = \mathbb{C}_e : (\varepsilon_e + \Delta \varepsilon)$ . The Jacobian of the residual vector respect to the variables is

$$\nabla \mathbf{R}^{[j]} = \begin{bmatrix} \frac{\partial^{t+\Delta t} r_{\dot{\gamma}}^{[j]}}{\partial^{t+\Delta t} \dot{\gamma}} & \frac{\partial^{t+\Delta t} r_{\gamma}^{[j]}}{\partial^{t+\Delta t} \gamma} \\ \frac{\partial^{t+\Delta t} r_f^{[j]}}{\partial^{t+\Delta t} \dot{\gamma}} & \frac{\partial^{t+\Delta t} r_f^{[j]}}{\partial^{t+\Delta t} \gamma} \end{bmatrix} \quad (134)$$

The first derivative is

$$\frac{\partial^{t+\Delta t} r_{\dot{\gamma}}}{\partial^{t+\Delta t} \dot{\gamma}} = 1 - \frac{t\dot{\gamma} - {}^{t+\Delta t}\dot{\gamma}_{\infty}}{t+\Delta t \hat{\tau}^2} \frac{d^{t+\Delta t} \hat{\tau}}{\partial^{t+\Delta t} \dot{\gamma}} \exp\left(-\frac{\Delta t}{t+\Delta t \hat{\tau}}\right) \quad (135)$$

with

$$\frac{\partial^{t+\Delta t} \hat{\tau}}{\partial^{t+\Delta t} \dot{\gamma}} := \frac{g''(t+\Delta t \dot{\gamma})}{t+\Delta t h} - \frac{g'(t+\Delta t \dot{\gamma})}{t+\Delta t h^2} \frac{\partial^{t+\Delta t} h}{\partial^{t+\Delta t} \dot{\gamma}} \quad (136)$$

so

$$\nabla \mathbf{R}_{11} \equiv \frac{\partial^{t+\Delta t} r_{\dot{\gamma}}}{\partial^{t+\Delta t} \dot{\gamma}} = 1 - \frac{t\dot{\gamma} - {}^{t+\Delta t}\dot{\gamma}_{\infty}}{t+\Delta t \hat{\tau}^2} \frac{g''(t+\Delta t \dot{\gamma})}{t+\Delta t h} \exp\left(-\frac{\Delta t}{t+\Delta t \hat{\tau}}\right) \quad (137)$$

where we used  $\partial {}^{t+\Delta t} \hat{\mathbf{n}} / \partial^{t+\Delta t} \dot{\gamma} = \mathbf{0}$ , and  $\partial^{t+\Delta t} h / \partial^{t+\Delta t} \dot{\gamma} = 0$  and  $\partial^{t+\Delta t} \dot{\gamma}_{\infty} / \partial^{t+\Delta t} \dot{\gamma} = 0$  (because they only depend on  ${}^{t+\Delta t} \gamma$ ) The second derivative is

$$\frac{\partial^{t+\Delta t} r_{\dot{\gamma}}}{\partial^{t+\Delta t} \dot{\gamma}} = -\frac{\partial^{t+\Delta t} \dot{\gamma}_{\infty}}{\partial^{t+\Delta t} \dot{\gamma}} \left[ 1 - \exp\left(-\frac{\Delta t}{t+\Delta t \hat{\tau}}\right) \right] - \frac{t\dot{\gamma} - {}^{t+\Delta t}\dot{\gamma}_{\infty}}{t+\Delta t \hat{\tau}^2} \frac{d^{t+\Delta t} \hat{\tau}}{\partial^{t+\Delta t} \dot{\gamma}} \exp\left(-\frac{\Delta t}{t+\Delta t \hat{\tau}}\right) \quad (138)$$

with  $\partial^{t+\Delta t} h / \partial^{t+\Delta t} \gamma = \kappa''(t+\Delta t \gamma)$  and

$$\frac{\partial {}^{t+\Delta t} \dot{\gamma}_{\infty}}{\partial^{t+\Delta t} \gamma} = -\frac{c {}^{t+\Delta t} \hat{\mathbf{n}} : \mathbb{C}_e : \Delta \varepsilon / \Delta t}{t+\Delta t h^2} \kappa''(t+\Delta t \gamma) \quad (139)$$

and

$$\frac{d^{t+\Delta t} \hat{\tau}}{\partial^{t+\Delta t} \gamma} = -\frac{g'(t+\Delta t \dot{\gamma})}{t+\Delta t h^2} \kappa''(t+\Delta t \gamma)$$

so

$$\begin{aligned} \nabla \mathbf{R}_{12} \equiv \frac{\partial^{t+\Delta t} r_{\gamma}}{\partial^{t+\Delta t} \gamma} &= c {}^{t+\Delta t} \hat{\mathbf{n}} : \mathbb{C}_e : \frac{\Delta \varepsilon}{\Delta t} \frac{\kappa''(t+\Delta t \gamma)}{t+\Delta t h^2} \left[ 1 - \exp\left(-\frac{\Delta t}{t+\Delta t \hat{\tau}}\right) \right] \\ &+ \frac{t\dot{\gamma} - {}^{t+\Delta t}\dot{\gamma}_{\infty}}{t+\Delta t \hat{\tau}^2} g'(t+\Delta t \dot{\gamma}) \frac{\kappa''(t+\Delta t \gamma)}{t+\Delta t h^2} \exp\left(-\frac{\Delta t}{t+\Delta t \hat{\tau}}\right) \end{aligned} \quad (140)$$



and note that since  $\Delta\gamma$  does not change the return direction (as previously anticipated) we get (and have used this result in the previous equations)  $\partial^{t+\Delta t}\hat{\mathbf{n}}/\partial^{t+\Delta t}\gamma = \mathbf{0}$ .

For the third derivative, note that  ${}^{tr}f$  does not depend on  ${}^{t+\Delta t}\dot{\gamma}$  nor on  ${}^{t+\Delta t}\gamma$ , so using the previous results, is

$$\nabla R_{21} \equiv \frac{\partial^{t+\Delta t} r_f}{\partial^{t+\Delta t} \gamma} = -c^2 {}^{t+\Delta t}\hat{\mathbf{n}} : \mathbb{C}_e : {}^{t+\Delta t}\hat{\mathbf{n}} - \kappa' ({}^{t+\Delta t}\gamma) \quad (141)$$

where we used

$$\frac{\partial^{t+\Delta t} \boldsymbol{\sigma}}{\partial^{t+\Delta t} \gamma} = \mathbb{C}_e : \frac{\partial^{t+\Delta t} \boldsymbol{\varepsilon}_e}{\partial^{t+\Delta t} \gamma} = -c \mathbb{C}_e : {}^{t+\Delta t}\hat{\mathbf{n}} \quad (142)$$

Finally, the fourth derivative, taking again into account the previous results, is

$$\nabla R_{22} \equiv \frac{\partial^{t+\Delta t} r_f}{\partial^{t+\Delta t} \dot{\gamma}} = -g' ({}^{t+\Delta t}\dot{\gamma}) \quad (143)$$

Obviously, for the linear proportional case, we must recover the exact solution explained in the previous sections. In this case

$$\begin{cases} \nabla R_{11} \equiv \frac{\partial^{t+\Delta t} r_{\dot{\gamma}}}{\partial^{t+\Delta t} \dot{\gamma}} = 1 - g'' ({}^{t+\Delta t}\dot{\gamma}) (\dots) = 1 \\ \nabla R_{12} \equiv \frac{\partial^{t+\Delta t} r_{\dot{\gamma}}}{\partial^{t+\Delta t} \gamma} = \kappa'' ({}^{t+\Delta t}\gamma) (\dots) = 0 \\ \nabla R_{21} \equiv \frac{\partial^{t+\Delta t} r_f}{\partial^{t+\Delta t} \gamma} = -2\mu c^2 - H \\ \nabla R_{22} \equiv \frac{\partial^{t+\Delta t} r_f}{\partial^{t+\Delta t} \dot{\gamma}} = -\eta \end{cases} \quad (144)$$

so inverting the matrix and solving for just an iteration (note that  ${}^{t+\Delta t}\dot{\gamma}_{\infty}$  is explicitly known at this point)

$$\begin{bmatrix} {}^{t+\Delta t}\dot{\gamma} \\ {}^{t+\Delta t}\gamma \end{bmatrix} = \begin{bmatrix} {}^t\dot{\gamma} \\ {}^t\gamma \end{bmatrix} + \begin{bmatrix} 1 & 0 \\ \tau & (2\mu c^2 + H)^{-1} \end{bmatrix} \begin{bmatrix} ({}^t\dot{\gamma} - {}^{t+\Delta t}\dot{\gamma}_{\infty}) \left[ 1 - \exp\left(-\frac{\Delta t}{\hat{\tau}}\right) \right] \\ {}^{tr}f \end{bmatrix} \quad (145)$$

we recover the solution for the linear case, in a well-conditioned manner (regardless of the value of  $\eta$ ), as expected, see Eqs. (52) and (60).

## 6.2. Tangent for global equilibrium iterations

In deriving the tangent, when changing the strain increment  $\Delta\boldsymbol{\varepsilon}$  we must guarantee that the two conditions  $r_{\dot{\gamma}} = 0$  and  $r_f = 0$  still hold. This means that, upon local convergence

$$\begin{cases} d^{t+\Delta t} r_f (\Delta\boldsymbol{\varepsilon}, {}^{t+\Delta t}\gamma (\Delta\boldsymbol{\varepsilon}), {}^{t+\Delta t}\dot{\gamma} (\Delta\boldsymbol{\varepsilon})) / d\Delta\boldsymbol{\varepsilon} = 0 \\ d^{t+\Delta t} r_{\dot{\gamma}} (\Delta\boldsymbol{\varepsilon}, {}^{t+\Delta t}\gamma (\Delta\boldsymbol{\varepsilon}), {}^{t+\Delta t}\dot{\gamma} (\Delta\boldsymbol{\varepsilon})) / d\Delta\boldsymbol{\varepsilon} = 0 \end{cases} \quad (146)$$

The rates are

$$\begin{aligned} \frac{d^{t+\Delta t} r_f}{d\Delta\epsilon} &= \frac{\partial^{t+\Delta t} r_f}{\partial\Delta\epsilon} + \frac{\partial^{t+\Delta t} r_f}{\partial^{t+\Delta t} \gamma} \frac{\partial^{t+\Delta t} \gamma}{\partial\Delta\epsilon} + \frac{\partial^{t+\Delta t} r_f}{\partial^{t+\Delta t} \dot{\gamma}} \frac{\partial^{t+\Delta t} \dot{\gamma}}{\partial\Delta\epsilon} \\ &= \underbrace{c \, {}^{t+\Delta t} \hat{\mathbf{n}} : \mathbb{C}_e + {}^{tr} \boldsymbol{\sigma}^d : \mathbb{P}_n : \mathbb{C}_e}_{d^{tr} f / d\Delta\epsilon} + \underbrace{\nabla R_{22} \frac{\partial^{t+\Delta t} \gamma}{\partial\Delta\epsilon} + \nabla R_{21} \frac{\partial^{t+\Delta t} \dot{\gamma}}{\partial\Delta\epsilon}}_{d\Delta^{ct} f / d\Delta\epsilon} = \mathbf{0} \end{aligned} \quad (147)$$

$$\begin{aligned} \frac{d^{t+\Delta t} r_{\dot{\gamma}}}{d\Delta\epsilon} &= \frac{\partial^{t+\Delta t} r_{\dot{\gamma}}}{\partial\Delta\epsilon} + \frac{\partial^{t+\Delta t} r_{\dot{\gamma}}}{\partial^{t+\Delta t} \gamma} \frac{\partial^{t+\Delta t} \gamma}{\partial\Delta\epsilon} + \frac{\partial^{t+\Delta t} r_{\dot{\gamma}}}{\partial^{t+\Delta t} \dot{\gamma}} \frac{\partial^{t+\Delta t} \dot{\gamma}}{\partial\Delta\epsilon} \\ &= \frac{\partial^{t+\Delta t} r_{\dot{\gamma}}}{\partial\Delta\epsilon} + \nabla R_{12} \frac{\partial^{t+\Delta t} \gamma}{\partial\Delta\epsilon} + \nabla R_{11} \frac{\partial^{t+\Delta t} \dot{\gamma}}{\partial\Delta\epsilon} \\ &= - \frac{\partial^{t+\Delta t} \dot{\gamma}_{\infty}}{\partial\Delta\epsilon} \left[ 1 - \exp \left( - \frac{\Delta t}{t+\Delta t \hat{\tau}} \right) \right] + \nabla R_{11} \frac{\partial^{t+\Delta t} \gamma}{\partial\Delta\epsilon} + \nabla R_{12} \frac{\partial^{t+\Delta t} \dot{\gamma}}{\partial\Delta\epsilon} = \mathbf{0} \end{aligned} \quad (148)$$

with

$$\begin{aligned} \frac{\partial^{t+\Delta t} \dot{\gamma}_{\infty} (\Delta\epsilon, {}^{t+\Delta t} \gamma)}{\partial\Delta\epsilon} &= \frac{c}{\Delta t \, {}^{t+\Delta t} h({}^{t+\Delta t} \gamma)} \left[ {}^{tr} \hat{\mathbf{n}} : \mathbb{C}_e + \frac{\Delta\epsilon^d}{\| {}^{tr} \mathbf{n} \|} : \mathbb{C}_e : \mathbb{P}_n : \mathbb{C}_e \right] \\ &= \frac{c}{\Delta t \, {}^{t+\Delta t} h({}^{t+\Delta t} \gamma)} \left[ 2\mu \, {}^{tr} \hat{\mathbf{n}} + \frac{(2\mu)^2}{\| {}^{tr} \mathbf{n} \|} \mathbb{P}_n : \Delta\epsilon^d \right] \end{aligned} \quad (149)$$

Both conditions give immediately the quantities  $\partial^{t+\Delta t} \gamma / \partial\Delta\epsilon$  and  $\partial^{t+\Delta t} \dot{\gamma} / \partial\Delta\epsilon$  by solving the system of equations

$$\begin{bmatrix} \nabla R_{11} & \nabla R_{12} \\ \nabla R_{21} & \nabla R_{22} \end{bmatrix} \begin{bmatrix} (\partial^{t+\Delta t} \dot{\gamma} / \partial\Delta\epsilon)^T \\ (\partial^{t+\Delta t} \gamma / \partial\Delta\epsilon)^T \end{bmatrix} = - \begin{bmatrix} - (\partial^{t+\Delta t} \dot{\gamma}_{\infty} / \partial\Delta\epsilon)^T \left[ 1 - \exp \left( - \frac{\Delta t}{t+\Delta t \hat{\tau}} \right) \right] \\ (c \, {}^{t+\Delta t} \hat{\mathbf{n}} : \mathbb{C}_e + {}^{tr} \boldsymbol{\sigma}^d : \mathbb{P}_n : \mathbb{C}_e)^T \end{bmatrix} \quad (150)$$

The stress tensor is given by

$${}^{t+\Delta t} \boldsymbol{\sigma} ({}^{t+\Delta t} \boldsymbol{\epsilon}_e (\Delta\epsilon, {}^{t+\Delta t} \gamma)) = \mathbb{C}_e : {}^{t+\Delta t} \boldsymbol{\epsilon}_e = \mathbb{C}_e : [{}^t \boldsymbol{\epsilon}_e + \Delta\epsilon - ({}^{t+\Delta t} \gamma - {}^t \gamma) \, {}^{tr} \hat{\mathbf{n}}] \quad (151)$$

so

$$\mathbb{C} := \frac{d \, {}^{t+\Delta t} \boldsymbol{\sigma} ({}^{t+\Delta t} \boldsymbol{\epsilon}_e (\Delta\epsilon, {}^{t+\Delta t} \gamma (\Delta\epsilon)))}{d\Delta\epsilon} = \mathbb{C}_e : \left[ \mathbb{I}^S - {}^{tr} \hat{\mathbf{n}} \otimes \frac{\partial^{t+\Delta t} \gamma}{\partial\Delta\epsilon} - \frac{\Delta\gamma}{\| {}^{tr} \mathbf{n} \|} \mathbb{P}_n : \mathbb{C}_e \right] \quad (152)$$

of which all quantities are known. We note that in contrast to that reported in [25] (see Sec. 4.2 therein), our algorithmic tangent is symmetric, the same way as those of inviscid plasticity and viscoelasticity.

### 6.3. Inviscid to viscous case

In this case it is also possible to compute the  $\Delta t^c$  such that the inviscid plastic yield surface is crossed. The procedure is similar to that developed for the linear case. However, assuming that we are dealing with a nonlinear case in which the solution will be approximate, a simpler acceptable procedure may be to just consider the step as fully viscoplastic (as e.g. in [25]), in which initially  ${}^t\dot{\gamma} = 0$  and in which finally  ${}^{t+\Delta t}f = 0$ . If the steps are small, the error induced in this step will also be small. Note that in this case, the consistent tangent for equilibrium iterations is the same as in the previous case.

### 6.4. Viscous to inviscid case

This case is detected by a result of a trial fully viscoplastic step in which  ${}^{t+\Delta t}\dot{\gamma} < 0$  and/or  ${}^{t+\Delta t}f_p \leq 0$  (note that because of the approximations in the nonlinear case, it is possible that both conditions are not met simultaneously). Then, for example, when the condition  ${}^{t+\Delta t}\dot{\gamma} < 0$  is detected, the step may be considered elastic, by simply setting  ${}^{t+\Delta t}\dot{\gamma} = 0$  and approximating  $\Delta\gamma$  by (in small steps it can also be taken  $\Delta\gamma \simeq 0$ )

$$\Delta\gamma \simeq \frac{{}^t f_p}{{}^t h({}^t\gamma + \hat{\tau}^t\dot{\gamma})} \quad (153)$$

In this case, the consistent tangent for equilibrium iterations is the elastic one  $\mathbb{C}_e$ .

## 7. Numerical examples

The purpose of this section is to show the numerical performance of the proposed algorithm in a typical finite element simulation using a nonlinear viscoplasticity model. A Perzyna-type nonlinear model for  $g(\dot{\gamma})$  is employed, see Eq. (106), so for the viscous contribution, a viscosity  $\bar{\eta}$  and the rate sensitivity parameter  $N$  are used (apart from the adimensionalizing parameter  $\bar{\kappa} = \kappa_0$ ). For the inviscid part  $\kappa(\gamma)$ , a Voce-type relation is employed. The parameters of the model are given in Table 2. The numerical example consists in the extension of a strip of thickness 1 mm with a central circular hole. It is presented to assess accuracy and robustness of the proposed viscoplasticity model and of the adopted numerical scheme. The strip is subjected to a loading simulated via imposed displacement in the vertical direction up to  $u/L = 0.32 \text{ mm}/16 \text{ mm}$ , where  $u$  is the prescribed displacement and  $L$  is the length of the specimen, see Fig. 10. The considered loading rates  $\dot{u}/L$  are 2.0/s, 1.0/s and 0.5/s. The analysis corresponds to only one quarter part of the plate, taking into account its symmetries. Figure 10 shows the geometry and the finite element discretization. High order mixed  $u/p$  fully integrated ( $3 \times 3 \times 3$  Gauss integration) Q2/P1 - 27/4 brick finite elements are used for this analysis.

The numerical solutions are obtained with our in-house finite element code Dulcinea. Figure 11 gives a comparison of the force-displacement curve between results obtained by changing the loading rate for two values of rate sensitivity  $\bar{N} = 1.0$  (a linear viscoplastic case) and  $N = 0.1$  (nonlinear viscoplastic case). The major influence of the loading rate is observed for the high rate-sensitive material as expected. For the low loading rate  $\dot{u}/L = 0.5$  and for low rate sensitivity  $N = 0.1$ , the obtained solution tends to the rate-independent solution, as expected.

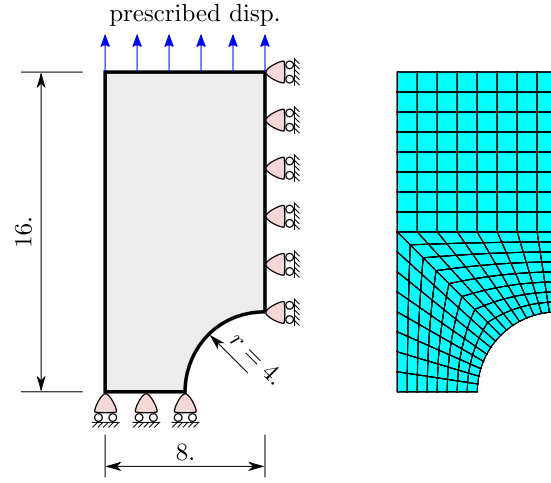


Figure 10: Strip with circular hole: geometry and FE model

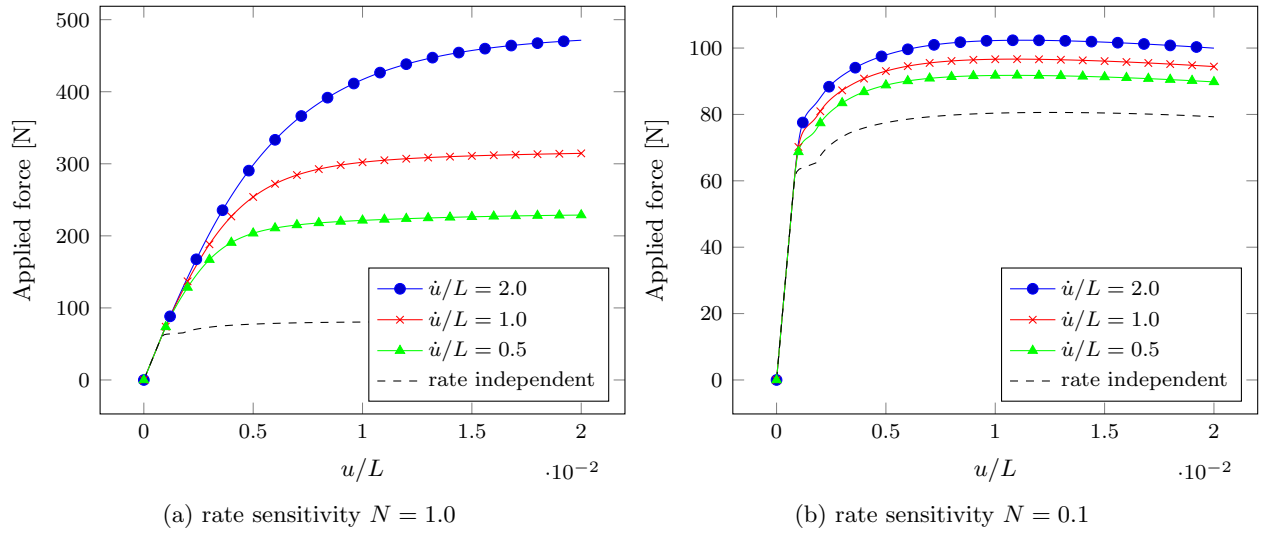


Figure 11: Force versus displacement curves for different loading rates

Table 2: Material parameters for the plate hole simulation. Voce's law is  $\kappa(\gamma) = \kappa_0 + H\gamma + (\kappa_\infty - \kappa_0) \exp(-\delta\gamma)$ . Perzyna's model employed is  $\dot{\gamma} = \langle f_p/\kappa_0 \rangle^N / \bar{\eta}$ , so  $g(\dot{\gamma}) = \kappa_0 \bar{\eta}^{1/N} \dot{\gamma}^{1/N}$ .

Young modulus	$E = 206.9$ GPa
Poisson coef.	$\nu = 0.29$
Reference yield stress	$\kappa_0 = 450.0$ MPa
Limit stress parameter	$\kappa_\infty = 550.0$ MPa
Hardening modulus	$\bar{H} = 200.0$ MPa
Voce exponential parameter	$\delta = 10$
Viscosity parameter	$\bar{\eta} = 1$ s

The von Mises stress contour at the final prescribed displacement is shown in Figure 12 for different loading rates. A higher von Mises stress level is observed for high loading rates as expected and it is in concordance with the force-displacement curve presented in Figure 11. Both local and global convergence rates are asymptotically quadratic, and typical values are given in Table 3 for different steps.

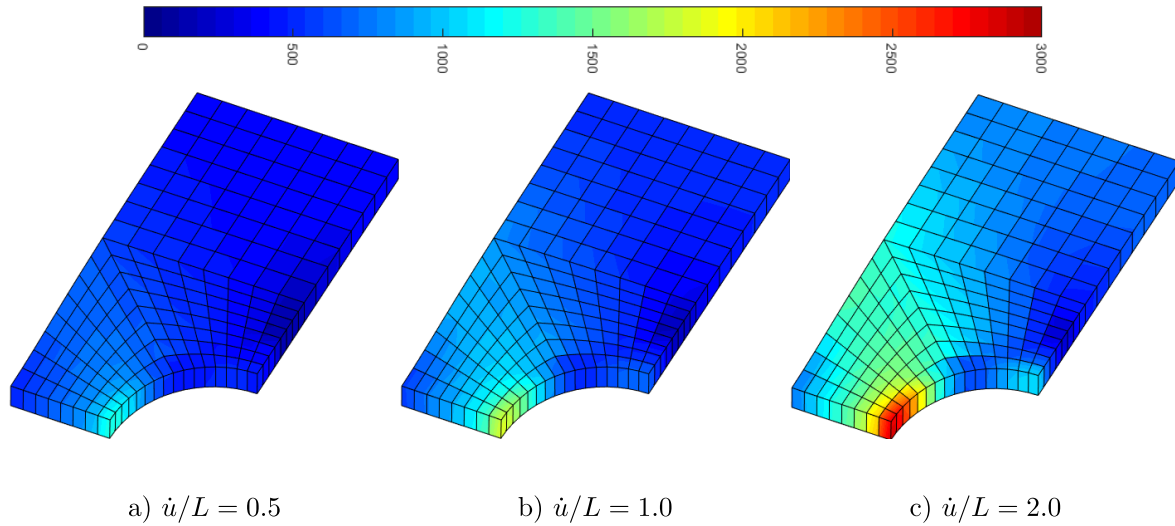


Figure 12: Stretching of the strip with circular hole: von Mises stress at final prescribed displacement for different loading rate.

## 8. Conclusions

In this work we present a novel treatment of viscoplasticity, both from a theoretical side and a computational one. One of our purposes has been to integrate exactly the linear proportional case in a manner such that the viscous behavior is constructed from the inviscid one in rate form, the latter recovered automatically for vanishing viscosities. However, we pursued a formulation also valid for more general nonlinear viscoplasticity cases which, fur-

Table 3: Extension of strip with circular hole. Convergence rates for global Newton-Raphson iterations (rnom= residual in force; enorm= residual in energy; R(•)= error in local equations)

Global convergence				
Iteration	Step 50		Step 200	
	rnorm	enorm	rnorm	enorm
1	$1.188E + 02$	$1.571E - 01$	$1.191E + 02$	$1.631E - 01$
2	$5.133E - 03$	$1.627E - 10$	$1.118E - 03$	$2.049E - 11$
3	$8.058E - 07$	$8.522E - 18$	$6.957E - 06$	$6.891E - 16$
Local convergence				
Iteration	R(1)		R(2)	
1	$1.323E + 01$		$3.924E + 01$	
2	$9.691E - 03$		$3.017E - 02$	
3	$4.425E - 10$		$4.133E - 09$	
4	$1.013E - 14$		$1.319E - 13$	

thermore, recovers the *viscoelastic* formulation for vanishing yield surfaces. The formulation unifies naturally the plasticity, viscoelasticity and viscoplasticity models and algorithms.

Essential to the developments has been the derivation of the evolution equations from thermodynamics, considering separately the conservation of power from the conservation of energy, the former yielding a constitutive equation for the equivalent viscoplastic strain rate, and the second one giving an extra equation for the computation of the equivalent viscoplastic strain. In the linear proportional case, the solution is exact for a given step. However, this setting also allows for a simple incorporation of the general nonlinear viscoplasticity models.

We have presented and analyzed the model and integration procedure using a small strains framework based on elastic corrector rates. As we have shown in previous works in anisotropic elastoplasticity and viscoelasticity, this framework can be easily extended to large strains employing classical multiplicative decompositions and logarithmic strains, still resulting in the same additive structure, and reducing large strains to kinematic pre- and post-processors.

## Acknowledgments

Partial financial support for this work has been given by Agencia Estatal de Investigación of Spain under grant PGC2018-097257-B-C32.

## References

- [1] K. M., K. Bathe, Inelastic analysis of solids and structures, Springer, 2005.
- [2] J. Lubliner, Plasticity Theory, Macmillan, 1990.
- [3] P. Perzyna, Fundamental Problems in Viscoplasticity, Advances in Applied Mechanics 9 (C) (1966) 243–377. doi:10.1016/S0065-2156(08)70009-7.

- [4] G. Duvaut, J. Lions, *Les Inequations en Mecanique et en Physique*, Dunod, Paris, 1972.
- [5] O. C. Zienkiewicz, I. C. Corneau, Visco-Plasticity-Plasticity and Creep in Elastic Solids - A unified numerical solution approach, *International Journal for Numerical Methods in Engineering* 8 (March) (1974) 821–845.
- [6] T. J. Hughes, R. L. Taylor, Unconditionally stable algorithms for quasi-static elasto/visco-plastic finite element analysis, *Computers and Structures* 8 (2) (1978) 169–173. doi:10.1016/0045-7949(78)90019-6.
- [7] I. Corneau, Numerical stability in quasistatic elasto/viscoplasticity, *International Journal for Numerical Methods in Engineering* 9 (1) (1975) 109–127. doi:10.1002/nme.1620090110.
- [8] J. C. Simo, J. G. Kennedy, S. Govindjee, Non-Smooth Multisurface Plasticity and Viscoplasticity . Loading / Unloading Conditions and Numerical Algorithms, *International Journal for Numerical Methods in Engineering* 26 (June 1987) (1988) 2161–2185.
- [9] J. L. Chaboche, Constitutive equations for cyclic plasticity and cyclic viscoplasticity, *International Journal of Plasticity* 5 (May) (1989) 247–302. doi:http://dx.doi.org/10.1016/0749-6419(89)90015-6.
- [10] D. Peric, On a class of constitutive equations in viscoplasticity: Formulation and computational issues, *International Journal for Numerical Methods in Engineering* 36 (8) (1993) 1365–1393. doi:10.1002/nme.1620360807.
- [11] M. Ristinmaa, N. S. Ottosen, Viscoplasticity based on an additive split of the conjugated forces, *European Journal of Mechanics, A/Solids* 17 (2) (1998) 207–235. doi:10.1016/S0997-7538(98)80083-1.
- [12] K. Runesson, M. Ristinmaa, L. Mahler, Comparison of viscoplasticity formats and algorithms, *Mechanics of Cohesive-Frictional Materials* 4 (1) (1999) 75–98. doi:10.1002/(SICI)1099-1484(199901)4:1<75::AID-CFM60>3.0.CO;2-4.
- [13] A. Caggiano, E. Martinelli, D. Said Schicchi, G. Etse, A modified Duvaut-Lions zero-thickness interface model for simulating the rate-dependent bond behavior of FRP-concrete joints, *Composites Part B: Engineering* 149 (April) (2018) 260–267. doi:10.1016/j.compositesb.2018.05.010.  
URL <https://doi.org/10.1016/j.compositesb.2018.05.010>
- [14] A. Ibrahimbegović, L. Chorfi, Viscoplasticity model at finite deformations with combined isotropic and kinematic hardening, *Computers and Structures* 77 (5) (2000) 509–525. doi:10.1016/S0045-7949(99)00232-1.
- [15] B. Nedjar, Frameworks for finite strain viscoelastic-plasticity based on multiplicative decompositions. Part I: Continuum formulations, *Computer Methods in Applied Mechanics and Engineering* 191 (15-16) (2002) 1541–1562. doi:10.1016/S0045-7825(01)00337-1.

- [16] A. V. Shutov, R. Kreißig, Finite strain viscoplasticity with nonlinear kinematic hardening: Phenomenological modeling and time integration, *Computer Methods in Applied Mechanics and Engineering* 197 (21-24) (2008) 2015–2029. [arXiv:0706.0429](#), [doi:10.1016/j.cma.2007.12.017](#).
- [17] K. Kowalczyk-Gajewska, E. A. Pieczyska, K. Golasinski, M. Maj, S. Kuramoto, T. Furutab, A finite strain elastic-viscoplastic model of Gum Metal, *International Journal of Plasticity* 119 (October 2018) (2019) 85–101. [doi:10.1016/j.ijplas.2019.02.017](#). URL <https://doi.org/10.1016/j.ijplas.2019.02.017>
- [18] H. Wang, P. Wu, C. Tomé, Y. Huang, A finite strain elastic-viscoplastic self-consistent model for polycrystalline materials, *Journal of the Mechanics and Physics of Solids* 58 (4) (2010) 594–612.
- [19] C. Miehe, J. Schröder, A comparative study of stress update algorithms for rate-independent and rate-dependent crystal plasticity, *International Journal for Numerical Methods in Engineering* 50 (2001) 273–298.
- [20] J. C. Simo, T. J. R. Hughes, *Computational inelasticity*, Springer, 1998.
- [21] E. A. de Souza-Neto, D. Perić, D. Owen, *Computational Methods for Plasticity: Theory and Applications*, Wiley, 2008.
- [22] W. M. Wang, L. J. Sluys, d. R. R. Borst, Viscoplasticity for instabilities due to strain softening and strain-rate softening, *International Journal for Numerical Methods in Engineering* 40 (20) (1997) 3839–3864. [doi:10.1002/\(SICI\)1097-0207\(19971030\)40:20<3839::AID-NME245>3.0.CO;2-6](#).
- [23] M. Ristinmaa, N. S. Ottosen, Consequences of dynamic yield surface in viscoplasticity, *International Journal of Solids and Structures* 37 (33) (2000) 4601–4622. [doi:10.1016/S0020-7683\(99\)00158-4](#).
- [24] A. Carosio, K. Willam, G. Etse, On the consistency of viscoplastic formulations, *International Journal of Solids and Structures* 37 (48) (2000) 7349–7369. [doi:10.1016/S0020-7683\(00\)00202-X](#).
- [25] O. M. Heeres, A. S. J. Suiker, R. De Borst, A comparison between the Perzyna viscoplastic model and the consistency viscoplastic model, *European Journal of Mechanics, A/Solids* 21 (1) (2002) 1–12. [doi:10.1016/S0997-7538\(01\)01188-3](#).
- [26] R. Zaera, J. Fernández-Sáez, An implicit consistent algorithm for the integration of thermoviscoplastic constitutive equations in adiabatic conditions and finite deformations, *International Journal of Solids and Structures* 43 (6) (2006) 1594–1612. [doi:10.1016/j.ijsolstr.2005.03.070](#).
- [27] M. Latorre, F. Montáns, A new class of plastic flow evolution equations for anisotropic multiplicative elastoplasticity based on the notion of a corrector elastic strain rate, *Applied Mathematical Modelling* 55 (2018) 716–740.



- [28] M. A. Sanz, F. Montáns, M. Latorre, Computational anisotropic hardening multiplicative elastoplasticity based on the corrector elastic logarithmic strain rate, *Computer Methods in Applied Mechanics and Engineering* 320 (2017) 82–121.
- [29] M. Sanz, K. Nguyen, M. Latorre, M. Rodríguez, F. Montáns, Sheet metal forming analysis using a large strain anisotropic multiplicative plasticity formulation, based on elastic correctors, which preserves the structure of the infinitesimal theory, *Finite Elements in Analysis and Design* 164 (2019) 1–17.
- [30] M. Zhang, F. Montáns, A simple formulation for large-strain cyclic hyperelasto-plasticity using elastic correctors. theory and algorithmic implementation, *International Journal of Plasticity* 113 (2019) 185–217.
- [31] K. Nguyen, M. Sanz, F. Montáns, Plane-stress constrained multiplicative hyperelasto-plasticity with nonlinear kinematic hardening. consistent theory based on elastic corrector rates and algorithmic implementation, *International Journal of Plasticity* In press, <https://doi.org/10.1016/j.ijplas.2019.08.017>.
- [32] C. Truesdell, W. Noll, *The Non-Linear Field Theories of Mechanics*, 3rd Ed., Springer, 2004.
- [33] M. Latorre, F. Montáns, Anisotropic finite strain viscoelasticity based on the sidoroff multiplicative decomposition and logarithmic strains, *Computational Mechanics* 56 (2016) 503–531.
- [34] M. Latorre, F. Montáns, Fully anisotropic finite strain viscoelasticity based on a reverse multiplicative decomposition and logarithmic strains, *Computers and Structures* 163 (2016) 56–70.
- [35] M. Latorre, F. Montáns, Bi-modulus materials consistent with a stored energy function: Theory and numerical implementation, *Computers and Structures* 229 (2020) 106176.
- [36] K.-J. Bathe, *Finite Element Procedures*, 2nd Ed., Klaus-Jürgen Bathe, 2014.
- [37] E. Dvorkin, M. Goldschmit, *Nonlinear Continua*, Springer, 2005.
- [38] M. L. Wilkins, Calculation of elastic-plastic flow, Tech. Rep. UCRL-7322, University of California, Lawrence Radiation Laboratory, Livermore (1963).
- [39] D. Perić, On a class of constitutive equations in viscoplasticity: formulation and computational issues, *International Journal for Numerical Methods in Engineering* 36 (1993) 1365–1393.